Chapter 5

Energy transport in stellar interiors

The energy that a star radiates from its surface is generally replenished from sources or reservoirs located in its hot central region. This represents an outward energy flux at every layer in the star, and it requires an effective means of transporting energy through the stellar material. This transfer of energy is possible owing to a non-zero temperature gradient in the star. While radiation is often the most important means of energy transport, and its is always present, it is not the only means. In stellar interiors, where matter and radiation are always in local thermodynamic equilibrium (Chapter 3) and the mean free paths of both photons and gas particles are extremely small, energy (heat) can be transported from hot to cool regions in two basic ways:

- Random thermal motions of the particles – either photons or gas particles – by a process that can be called *heat diffusion*. In the case of photons, the process is known as *radiative diffusion*. In the case of gas particles (atoms, ions, electrons) it is usually called *heat conduction*.
- Collective (bulk) motions of the gas particles, which is known as *convection*. This is an important process in stellar interiors, not only because it can transport energy very efficiently, it also results in rapid mixing. Unfortunately, convection is one of the least understood ingredients of stellar physics.

The transport of energy in stars is the subject of this chapter, which will lead us to two additional differential equations for the stellar structure.

5.1 Local energy conservation

In Chapter 2 we considered the global energy budget of a star, regulated by the virial theorem. We have still to take into account the conservation of energy on a local scale in the stellar interior. To do this we turn to the first law of thermodynamics (Sect. 3.4), which states that the internal energy of a system can be changed by two forms of energy transfer: heat and work. By δf we denote a change in a quantity f occurring in a small time interval δt. For a gas element of unit mass the first law can be written as (see eq. 3.47)

$$\delta u = \delta q + \frac{P}{\rho^2}\,\delta\rho. \tag{5.1}$$

The first term is the heat added or extracted, and second term represents the work done on (or performed by) the element. We note that compression ($\delta\rho > 0$) involves an addition of energy, and expansion is achieved at the expense of the element's own energy.

Consider a spherical, Lagrangian shell inside the star of constant mass Δm. Changes in the heat content of the shell ($\delta Q = \delta q\,\Delta m$) can occur due to a number of sources and sinks:

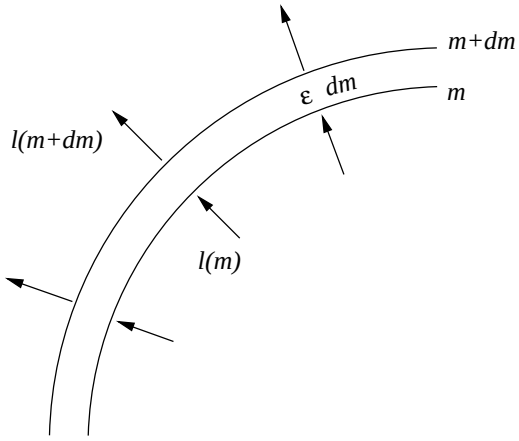

Figure 5.1. Energy generation and heat flow into and out of a spherical mass shell.

- Heat is added by the release of nuclear energy, if available. The rate at which nuclear energy is produced per unit mass and per second is written as $\epsilon_{\rm nuc}$. The details of nuclear energy generation will be treated in Chapter 6.

- Heat can be removed by the release of energetic neutrinos, which escape from the stellar interior without interaction. Neutrinos are released as a by-product of some nuclear reactions, in which case they are often accounted for in $\epsilon_{\rm nuc}$. But neutrinos can also be released by weak interaction processes in very hot and dense plasmas. This type of neutrino production plays a role in late phases of stellar evolution, and the rate at which these neutrinos take away energy per unit mass is written as ϵ_ν.

- Finally, heat is absorbed or emitted according to the balance of heat fluxes flowing into and out of the shell. We define a new variable, the *local luminosity* l, as the rate at which energy in the form of heat flows outward through a sphere of radius r (see Fig. 5.1). In spherical symmetry, l is related to the radial energy flux F (in erg s^{-1} cm^{-2}) as

$$l = 4\pi r^2 F. \tag{5.2}$$

  Therefore at the surface $l = L$ while at the centre $l = 0$. Normally heat flows outwards, in the direction of decreasing temperature. Therefore l is usually positive, but under some circumstances (e.g. cooling of central regions by neutrino emission) heat can flow inwards, meaning that l is negative. (We note that the energy flow in the form of neutrinos is treated separately and is *not* included in the definition of l and of the stellar luminosity L.)

We can therefore write:

$$\delta Q = \epsilon_{\rm nuc}\,\Delta m\,\delta t - \epsilon_\nu\,\Delta m\,\delta t + l(m)\,\delta t - l(m+\Delta m)\,\delta t,$$

with $l(m+\Delta m) = l(m) + (\partial l/\partial m)\cdot\Delta m$, so that after dividing by Δm,

$$\delta q = \left(\epsilon_{\rm nuc} - \epsilon_\nu - \frac{\partial l}{\partial m}\right)\delta t. \tag{5.3}$$

Combining eqs. (5.3) and (5.1) and taking the limit $\delta t \to 0$ yields:

$$\boxed{\frac{\partial l}{\partial m} = \epsilon_{\rm nuc} - \epsilon_\nu - \frac{\partial u}{\partial t} + \frac{P}{\rho^2}\frac{\partial \rho}{\partial t}} \tag{5.4}$$

This is the third equation of stellar evolution. The terms containing time derivatives are often combined into a function $\epsilon_{\rm gr}$:

$$\begin{aligned} \epsilon_{\rm gr} &= -\frac{\partial u}{\partial t} + \frac{P}{\rho^2}\frac{\partial \rho}{\partial t} \\ &= -T\frac{\partial s}{\partial t} \end{aligned} \tag{5.5}$$

where s is the specific entropy of the gas. One can then write

$$\frac{\partial l}{\partial m} = \epsilon_{\rm nuc} - \epsilon_\nu + \epsilon_{\rm gr} \tag{5.6}$$

If $\epsilon_{\rm gr} > 0$, energy is released by the mass shell, typically in the case of contraction. If $\epsilon_{\rm gr} < 0$, energy is absorbed by the shell, typically in the case of expansion.

In *thermal equilibrium* (see Sec. 2.3.2), the star is in a stationary state and the time derivatives vanish ($\epsilon_{\rm gr} = 0$). We then obtain a much simpler stellar structure equation,

$$\frac{{\rm d}l}{{\rm d}m} = \epsilon_{\rm nuc} - \epsilon_\nu. \tag{5.7}$$

If we integrate this equation over the mass we obtain

$$L = \int_0^M \epsilon_{\rm nuc}\,{\rm d}m - \int_0^M \epsilon_\nu\,{\rm d}m \equiv L_{\rm nuc} - L_\nu \tag{5.8}$$

which defines the nuclear luminosity $L_{\rm nuc}$ and the neutrino luminosity L_ν. Neglecting the neutrino losses for the moment, we see that thermal equilibrium implies that $L = L_{\rm nuc}$, that is, energy is radiated away at the surface at the same rate at which it is produced by nuclear reactions in the interior. This is indeed what we defined as thermal equilibrium in Sec. 2.3.2.

5.2 Energy transport by radiation and conduction

We have seen that most stars are in a long-lived state of thermal equilibrium, in which energy generation in the stellar centre exactly balances the radiative loss from the surface. What would happen if the nuclear energy source in the centre is suddenly quenched? The answer is: very little, at least initially. Photons that carry the energy are continually scattered, absorbed and re-emitted in random directions. Because stellar matter is very *opaque* to radiation, the photon mean free path $\ell_{\rm ph}$ is very small (typically $\ell_{\rm ph} \sim 1\,{\rm cm} \ll R_\odot$, see Sect. 3.1). As a result, radiation is trapped within the stellar interior, and photons diffuse outwards very slowly by a 'random walk' process. The time it takes radiation to escape from the centre of the Sun by this random walk process is roughly 10^7 years, despite the fact that photons travel at the speed of light (see Exercise 5.1). Changes in the Sun's luminosity would only occur after millions of years, on the timescale for radiative energy transport, which you may recognise as the Kelvin-Helmholtz timescale for thermal readjustment.

We also estimated in Sec. 3.1 that the temperature difference over a distance $\ell_{\rm ph}$ is only $\Delta T \sim 10^{-4}\,{\rm K}$. This means that the radiation field is extremely close to black-body radiation with $U = u\rho = aT^4$ (Sec. 3.3.6). Black-body radiation is isotropic and as a result no net energy transport would take place. However, a small anisotropy is still present due to the tiny relative temperature difference $\Delta T/T \sim 10^{-11}$. This small anisotropy is enough to carry the entire energy flux in the Sun (see Exercise 5.1). These estimates show that radiative energy transport in stellar interiors can be described as a diffusion process. This yields a great simplification of the physical description.

5.2.1 Heat diffusion by random motions

Fick's law of diffusion states that, when there is a gradient $\boldsymbol{\nabla} n$ in the density of particles of a certain type, the diffusive flux $\boldsymbol{J}$ – i.e. the net flux of such particles per unit area per second – is given by

$$\boldsymbol{J} = -D\,\boldsymbol{\nabla} n \qquad \text{with} \qquad D = \tfrac{1}{3}\bar{v}\ell. \tag{5.9}$$

Here D is the *diffusion coefficient*, which depends on the average particle velocity $\bar{v}$ and their mean free path ℓ. The origin of this equation can be understood as follows.

Consider a unit surface area and particles crossing the surface in either direction. Let z be a coordinate in the direction perpendicular to the surface. The number of particles crossing in the positive z direction (say upward) per unit area per second is

$$\frac{\mathrm{d}N}{\mathrm{d}t} = \tfrac{1}{6} n \bar{v},$$

The factor $\frac{1}{6}$ comes from the fact that half of the particles cross the surface in one direction, and because their motions are isotropic the average velocity perpendicular to the surface is $\frac{1}{3}\bar{v}$ (this can be proven in the same way as the factor $\frac{1}{3}$ appearing in the pressure integral eq. 3.4). If there is a gradient in the particle density along the z direction, $\partial n/\partial z$, then the particles moving upwards with mean free path ℓ on average have a density $n(z-\ell)$ and those moving down on average have a density $n(z+\ell)$. Therefore the net particle flux across the surface is

$$J \;=\; \tfrac{1}{6}\bar{v}\,n(z-\ell) - \tfrac{1}{6}\bar{v}\,n(z+\ell) \;=\; \tfrac{1}{6}\bar{v}\cdot\Big(-2\ell\,\frac{\partial n}{\partial z}\Big) \;=\; -\tfrac{1}{3}\bar{v}\ell\,\frac{\partial n}{\partial z}.$$

Eq. (5.9) is the generalisation of this expression to three dimensions.

Suppose now that, in addition to a gradient in particle density, there is a gradient in the energy density U carried by these particles (e.g. photons or gas particles). Then by analogy, there is a net flux of energy across the surface, since the particles moving 'up' on average carry more energy than those moving 'down'. Therefore a gradient in the energy density $\boldsymbol{\nabla} U$ gives rise to a net energy flux

$$\boldsymbol{F} = -D\,\boldsymbol{\nabla} U, \tag{5.10}$$

Since a gradient in energy density is associated with a temperature gradient, $\boldsymbol{\nabla} U = (\partial U/\partial T)_V\,\boldsymbol{\nabla} T = C_V\,\boldsymbol{\nabla} T$, we can write this as an equation for heat conduction,

$$\boldsymbol{F} = -K\,\boldsymbol{\nabla} T \qquad \text{with} \qquad K = \tfrac{1}{3}\bar{v}\ell\,C_V, \tag{5.11}$$

where K is the *conductivity*. This description is valid for all particles in LTE, photons as well as gas particles.

5.2.2 Radiative diffusion of energy

For photons, we can take $\bar{v} = c$ and $U = aT^4$. Hence the specific heat (per unit volume) is $C_V = \mathrm{d}U/\mathrm{d}T = 4aT^3$. The photon mean free path can be obtained from the equation of radiative transfer, which states that the intensity I_ν of a radiation beam (in a medium without emission) is diminished over a length s by

$$\frac{\mathrm{d}I_\nu}{\mathrm{d}s} = -\kappa_\nu \rho\, I_\nu, \tag{5.12}$$

where κ_ν is the mass absorption coefficient or opacity coefficient (in $\mathrm{cm}^2\ \mathrm{g}^{-1}$) at frequency ν. The mean free path is the distance over which the intensity decreases by a factor of e, which obviously

depends on the frequency. If we make a proper average over frequencies (see Sec. 5.2.3), we can write

$$\ell_{\rm ph} = \frac{1}{\kappa\rho}. \tag{5.13}$$

The quantity κ is simply called the *opacity*. We can then compute the radiative conductivity

$$K_{\rm rad} = \tfrac{4}{3}\frac{acT^3}{\kappa\rho}, \tag{5.14}$$

such that the radiative energy flux is

$$\boldsymbol{F}_{\rm rad} = -K_{\rm rad}\,\boldsymbol{\nabla}T = -\tfrac{4}{3}\frac{acT^3}{\kappa\rho}\boldsymbol{\nabla}T. \tag{5.15}$$

In spherical symmetric star the flux is related to the local luminosity, $F_{\rm rad} = l/4\pi r^2$ (eq. 5.2). We can thus rearrange the equation to obtain the temperature gradient

$$\frac{\partial T}{\partial r} = -\frac{3\kappa\rho}{16\pi acT^3}\frac{l}{r^2} \tag{5.16}$$

or when combined with eq. (2.6) for $\partial r/\partial m$,

$$\boxed{\frac{\partial T}{\partial m} = -\frac{3}{64\pi^2 ac}\frac{\kappa l}{r^4T^3}} \tag{5.17}$$

This is the temperature gradient required to carry the entire luminosity l by radiation. It gives the fourth stellar structure equation, for the case that energy is transported only by radiation. A star, or a region inside a star, in which this holds is said to be in *radiative equilibrium*, or simply *radiative*.

Eq. (5.17) is valid as long as $\ell_{\rm ph} \ll R$, i.e. as long as the LTE conditions hold. This breaks down when the stellar surface, the photosphere, is approached: this is where the photons escape, i.e. $\ell_{\rm ph} \gtrsim R$. Near the photosphere the diffusion approximation is no longer valid and we need to solve the full, and much more complicated, equations of radiative transfer. This is the subject of the study of *stellar atmospheres*. Fortunately, the LTE conditions and the diffusion approximation hold over almost the entire stellar interior.

In hydrostatic equilibrium, we can combine eqs. (5.17) and (2.13) as follows

$$\frac{{\rm d}T}{{\rm d}m} = \frac{{\rm d}P}{{\rm d}m}\cdot\frac{{\rm d}T}{{\rm d}P} = -\frac{Gm}{4\pi r^4}\,\frac{T}{P}\cdot\frac{{\rm d}\log T}{{\rm d}\log P}$$

so that we can define the dimensionless *radiative temperature gradient*

$$\boxed{\nabla_{\rm rad} = \left(\frac{{\rm d}\log T}{{\rm d}\log P}\right)_{\rm rad} = \frac{3}{16\pi acG}\frac{\kappa lP}{mT^4}} \tag{5.18}$$

This describes the logarithmic variation of T with depth (where depth is now expressed by the *pressure*) for a star in HE if energy is transported only by radiation.

5.2.3 The Rosseland mean opacity

The radiative diffusion equations derived above are independent of frequency ν, since the flux F is integrated over all frequencies. However, in general the opacity coefficient κ_ν depends on frequency, such that the κ appearing in eq. (5.16) or (5.17) must represent a proper average over frequency. This average must be taken in a particular way.

If $\boldsymbol{F}_\nu\, d\nu$ represents the radiative flux in the frequency interval $[\nu, \nu + d\nu]$, then eq. (5.10) must be replaced by

$$\boldsymbol{F}_\nu = -D_\nu\, \boldsymbol{\nabla} U_\nu = -D_\nu\, \frac{\partial U_\nu}{\partial T}\, \boldsymbol{\nabla} T \tag{5.19}$$

where

$$D_\nu = \tfrac{1}{3} c \ell_\nu = \frac{c}{3\kappa_\nu \rho}. \tag{5.20}$$

The energy density U_ν in the same frequency interval follows from eq. (3.41), $U_\nu = h\nu\, n(\nu)$,

$$U_\nu = \frac{8\pi h}{c^3}\, \frac{\nu^3}{e^{h\nu/kT} - 1} \tag{5.21}$$

which is proportional to the Planck function for the intensity of black-body radiation. The total flux is obtained by integrating eq. (5.19) over all frequencies,

$$\boldsymbol{F} = -\Big[\frac{c}{3\rho} \int_0^\infty \frac{1}{\kappa_\nu} \frac{\partial U_\nu}{\partial T}\, \mathrm{d}\nu\Big]\, \boldsymbol{\nabla} T. \tag{5.22}$$

This is eq. (5.11) but with conductivity

$$K_{\rm rad} = \frac{c}{3\rho} \int_0^\infty \frac{1}{\kappa_\nu} \frac{\partial U_\nu}{\partial T}\, \mathrm{d}\nu. \tag{5.23}$$

Comparing with eq. (5.14) shows that the proper average of opacity as it appears in eq. (5.16) or (5.17) is

$$\frac{1}{\kappa} = \frac{1}{4aT^3} \int_0^\infty \frac{1}{\kappa_\nu} \frac{\partial U_\nu}{\partial T}\, \mathrm{d}\nu. \tag{5.24}$$

This is the so-called *Rosseland mean opacity*. The factor $4aT^3$ appearing in eq. (5.24) is equal to $\int_0^\infty (\partial U_\nu/\partial T)\, \mathrm{d}\nu$, so that the Rosseland mean can be seen as the harmonic mean of κ_ν with weighting function $\partial U_\nu/\partial T$. (The weighting function has a maximum at $h\nu \approx 4kT$, as can be verified by differentiating eq. (5.21) with respect to T, and subsequently with respect to ν.)

We can interpret the Rosseland mean in another way. The integrand of eq. (5.24) also appears in the expression (5.19) for the monochromatic flux, $\boldsymbol{F}_\nu$, when combined with (5.20). The Rosseland mean therefore favours the frequency range where the flux is large. In other words, $1/\kappa$ represents the average *transparency* of the stellar gas.

5.2.4 Conductive transport of energy

Collisions between the gas particles (ions and electrons) can also transport heat. Under normal (ideal gas) conditions, however, the collisional conductivity is very much smaller than the radiative conductivity. The collisional cross sections are typically $10^{-18} - 10^{-20}\,\mathrm{cm}^2$ at the temperatures in stellar interiors, giving a mean free path for collisions that is several orders of magnitude smaller than $\ell_{\rm ph}$. Furthermore the average particle velocity $\bar{v} = \sqrt{3kT/m} \ll c$. So normally we can neglect heat conduction compared to radiative diffusion of energy.

However, the situation can be quite different when the electrons become degenerate. In that case both their velocities increase (their momenta approach the Fermi momentum, see Sec. 3.3.5) and, more importantly, their mean free paths increase (most of the quantum cells of phase space are occupied, so an electron has to travel further to find an empty cell and transfer its momentum). At very high densities, when $\ell_e \gg \ell_{\rm ph}$, electron conduction becomes a much more efficient way of transporting energy than radiative diffusion (see Sec. 5.3). This is important for stars in late stages of evolution with dense degenerate cores and for white dwarfs, in which efficient electron conduction results in almost isothermal cores.

The energy flux due to heat conduction can be written as

$$\boldsymbol{F}_{\rm cd} = -K_{\rm cd}\,\boldsymbol{\nabla} T \tag{5.25}$$

such that the sum of radiative and conductive fluxes is

$$\boldsymbol{F} = \boldsymbol{F}_{\rm rad} + \boldsymbol{F}_{\rm cd} = -(K_{\rm rad} + K_{\rm cd})\,\boldsymbol{\nabla} T. \tag{5.26}$$

We can define a *conductive opacity* $\kappa_{\rm cd}$ by analogy with the radiative opacity, if we write the conductivity in the same form as eq. (5.14),

$$K_{\rm cd} = \frac{4acT^3}{3\kappa_{\rm cd}\,\rho}. \tag{5.27}$$

Then we can write the combined flux due to radiation and conduction in the same form as the radiative flux, eq. (5.15),

$$\boldsymbol{F} = -\frac{4acT^3}{3\kappa\rho}\boldsymbol{\nabla} T \qquad \text{with} \qquad \frac{1}{\kappa} = \frac{1}{\kappa_{\rm rad}} + \frac{1}{\kappa_{\rm cd}} \tag{5.28}$$

This result simply means that the transport mechanism with the largest flux will dominate, that is, the mechanism for which the stellar matter has the highest transparency. With κ defined as in eq. (5.28), the stellar structure equation (5.17) also accounts for the effects of conduction, if present.

5.3 Opacity

The opacity coefficient κ appearing in eq. (5.17) determines the flux that can be transported by radiation for a certain temperature gradient, or more to the point, how large the temperature gradient must be in order to carry a given luminosity l by radiation. Therefore κ is an important quantity that has a large effect on the structure of a star.

5.3.1 Sources of opacity

In the following subsections we briefly describe the different physical processes that contribute to the opacity in stellar interiors, and give some simple approximations.

Electron scattering

An electromagnetic wave that passes an electron causes it to oscillate and radiate in other directions, like a classical dipole. This scattering of the incoming wave is equivalent to the effect of absorption, and can be described by the Thomson cross-section of an electron

$$\sigma_{\rm e} = \frac{8\pi}{3}\left(\frac{e^2}{m_{\rm e}c^2}\right)^2 = 6.652\times10^{-25}\,{\rm cm}^2 \tag{5.29}$$

The associated opacity coefficient is due to the combined cross-section of all electrons in a unit mass of gas, which is obtained by dividing $\sigma_{\rm Th}$ by $\rho/n_{\rm e} = \mu_{\rm e} m_{\rm u}$,

$$\kappa_{\rm es} = \frac{\sigma_{\rm e}}{\mu_{\rm e} m_{\rm u}} = 0.20\,(1+X)\ \ {\rm cm}^2/{\rm g} \tag{5.30}$$

Since the electron scattering opacity is independent of frequency, this expression also gives the Rosseland mean. In the last equality we have assumed that the gas is completely ionized so that $\mu_{\rm e} = 2/(1+X)$ (eq. 3.20). Electron scattering is an important opacity source in an ionized gas that is not too dense. When the degree of ionization drops (typically when $T \lesssim 10^4$ K in hydrogen-rich gas) the electron density becomes so small that the electron scattering opacity is strongly reduced below eq. (5.30).

When the photon energy becomes a significant fraction of the rest mass of the electron, $h\nu \gtrsim 0.1 m_e c^2$, the exchange of momentum between photon and electron must be taken into account (Compton scattering). This occurs at high temperature, since the Planck function has a maximum at $h\nu = 4.965\,kT$ (Wien's law), i.e. when $kT \gtrsim 0.02 m_e c^2$ or $T \gtrsim 10^8$ K. At such temperatures the electron scattering opacity is smaller than given by eq. (5.30).

Free-free absorption

A free electron cannot absorb a photon because this would violate momentum and energy conservation. However, if a charged ion is in its vicinity, absorption is possible because of the electromagnetic coupling between the ion and electron. This *free-free absorption* is the inverse process of bremsstrahlung, where an electron emits a photon when it passes by and interacts with an ion.

The full derivation of the absorption coefficient for this process is a quantum-mechanical problem. However, an approximate calculation has been done classically by Kramers. He derived that the absorption efficiency of such a temporary electron-ion system is proportional to $Z_i{}^2 \nu^{-3}$, where Z_i is the charge of the ion. To obtain the cross-section of a certain ion i, this has to be multiplied by the electron density $n_{\rm e}$ and by the time during which the electron and ion will be close enough for the coupling to occur. This can be estimated from the mean velocity of the electrons, $\overline{v} = (3kT/m_{\rm e})^{1/2}$, so that $\Delta t \propto 1/\overline{v} \propto T^{-1/2}$, i.e. $\sigma_{{\rm ff},i} \propto n_{\rm e} T^{-1/2} Z_i{}^2 \nu^{-3}$. The opacity coefficient follows by multiplying the cross section by n_i/ρ, where n_i is the ion number density, and summing over all ions in the mixture:

$$\kappa_{\nu,{\rm ff}} \propto \frac{n_{\rm e}}{\rho} \sum_i n_i\, Z_i{}^2\, T^{-1/2}\, \nu^{-3}.$$

In a completely ionized gas, $n_{\rm e}/\rho = 1/(\mu_{\rm e} m_{\rm u}) = (1+X)/2m_{\rm u}$. Following Sec. 3.3.3, the sum over ions can be written as $\sum_i n_i Z_i{}^2 = (\rho/m_{\rm u}) \sum_i (X_i Z_i{}^2/A_i) = (\rho/m_{\rm u})\,(X+Y+B)$, where $B = \sum_{i>2} (X_i Z_i{}^2/A_i)$ is the contribution of elements heavier than helium. As long as their abundance is small, one can take $X + Y + B \approx 1$ to a reasonable approximation.

When we take the Rosseland mean, the factor ν^{-3} becomes a factor T^{-3} (this can be verified by performing the integration of eq. 5.24 with $\kappa_\nu \propto \nu^{-\alpha}$, see Exercise 5.2). We thus obtain

$$\kappa_{\rm ff} \propto \rho\, T^{-7/2}. \tag{5.31}$$

An opacity law of this form is called *Kramers opacity*. Putting in the numerical factors and the compositional dependence for an ionized gas, the following approximate expression is obtained,

$$\kappa_{\rm ff} \approx 3.8 \times 10^{22}\,(1+X)\,\rho\, T^{-7/2}\ \ {\rm cm}^2/{\rm g}. \tag{5.32}$$

N.B. This formula should be used with caution: it can give some insight in simplifying approaches but should not be used in serious applications. One omission is a correction factor for quantum-mechanical effects, the so-called Gaunt factor $g_{\rm ff}$.

Bound-free and bound-bound absorption

Bound-free absorption is the absorption of a photon by a bound electron whereby the photon energy exceeds the ionization energy χ of the ion or atom. Computing the opacity due to this process requires carefully taking into account the atomic physics of all the ions and atoms present in the mixture, and is thus very complicated. Classical considerations, similar to those for free-free absorption, show that the frequency dependence is again $\propto \nu^{-3}$, as long as $h\nu > \chi_{\rm ion}$. Therefore, in rough approximation the total bound-free opacity is also of the Kramers form. A very approximate formula is

$$\kappa_{\rm bf} \approx 4.3 \times 10^{25}\,(1+X)Z\,\rho\,T^{-7/2}\ \ {\rm cm}^2/{\rm g}. \tag{5.33}$$

Again one should use this formula with caution. It should certainly not be applied for $T \lesssim 10^4\,{\rm K}$ because most of the photons are not energetic enough to ionize the electrons, while at very high T most species are fully ionized so the bound-free opacity is smaller than eq. (5.33) suggests. Keeping these limitations in mind, the bound-free opacity is seen to depend directly on the metallicity Z. One thus has, very approximately, $\kappa_{\rm bf} \approx 10^3 Z \times \kappa_{\rm ff}$. We may thus expect bound-free absorption to dominate over free-free absorption for $Z \gtrsim 10^{-3}$.

Bound-bound absorption is related to photon-induced transitions between bound states in atoms or ions. Although this is limited to certain transition frequencies, the process can be efficient because the absorption lines are strongly broadened by collisions. Again, the computation of opacity is complex because one has to include a detailed treatment of line profiles under a wide variety of conditions. Bound-bound absorption is mainly important for $T \lesssim 10^6\,{\rm K}$, at higher temperatures its contribution to the total opacity is small.

The negative hydrogen ion

An important source of opacity in relatively cool stars (e.g. in the solar atmosphere) is formed by bound-free absorption of the negative hydrogen ion H^-. Neutral hydrogen is easily polarized by a nearby charge and can then form a bound state with another electron, with an ionization potential of 0.75 eV. The resulting H^- is very fragile and is easily ionized at temperatures of a few thousand K. However, to make the ion requires the presence of both neutral hydrogen and free electrons. The free electrons come mainly from singly ionized metals such as Na, K, Ca or Al. The resulting opacity is therefore sensitive to metallicity and to temperature. A very approximate formula in the range $T \sim (3-6)\times 10^3\,{\rm K}$, $\rho \sim (10^{-10} - 10^{-5})\,{\rm g/cm}^3$ and $0.001 < Z < 0.02$ is

$$\kappa_{\rm H^-} \approx 2.5 \times 10^{-31} \left(\frac{Z}{0.02}\right) \rho^{1/2}\,T^9\ \ {\rm cm}^2/{\rm g} \tag{5.34}$$

At very low metal abundance and/or $T \lesssim 3000\,{\rm K}$ the H^- opacity becomes ineffective. At $T \gtrsim 10^4\,{\rm K}$ most of the H^- has disappeared and the Kramers opacity and electron scattering take over.

Molecules and dust

In cool stars with $T_{\rm eff} \lesssim 4000\,{\rm K}$ opacity sources arising from molecules and (at even lower temperatures) dust grains become dominant. Here one has to deal with complicated molecular chemistry and dust formation processes, which still contains a lot of uncertainty. When dust grains form, at $T \lesssim 1500\,{\rm K}$, they are very effective absorbers in the outer atmospheres of very cool stars.

Conductive opacities

As we saw in Sec. 5.2.4, energy transport by means of heat conduction can also be described by means of a conductive opacity coefficient $\kappa_{\rm cd}$. Under ideal gas conditions, conduction is very inefficient

compared to radiative transport of energy ($\kappa_{\rm cd} \gg \kappa_{\rm rad}$). Therefore we only need to consider the case of a degenerate electron gas. In this case the following approximation holds

$$\kappa_{\rm cd} \approx 4.4 \times 10^{-3} \, \frac{\sum_i Z_i^{5/3} X_i / A_i}{(1+X)^2} \, \frac{(T/10^7\,{\rm K})^2}{(\rho/10^5\,{\rm g/cm^3})^2} \;\; {\rm cm^2/g}. \tag{5.35}$$

At high densities and low temperatures, the conductive opacity becomes very small because of the large electron mean free path in a highly degenerate gas. This is why degenerate stellar regions are highly conductive and rapidly become isothermal.

5.3.2 A detailed view of stellar opacities

In general, $\kappa = \kappa(\rho, T, X_i)$ is a complicated function of density, temperature and composition. While certain approximations can be made, as in the examples shown above, these are usually too simplified and inaccurate to apply in detailed stellar models. An additional complication is that the Rosseland mean opacity (eq. 5.24) is not additive: the opacity of a mixture of gases is not simply equal to the sum of the opacities of its components. Instead, one first has to add the frequency-dependent opacities, $\kappa_\nu = \sum_i X_i \kappa_{\nu,i}$ and then integrate over ν to calculate the Rosseland mean.

In practical stellar structure calculations one usually interpolates in pre-computed opacity tables, e.g. as calculated in the 1990s by the OPAL project. An example is shown in Fig. 5.2 for a quasi-solar mixture of elements. One may recognize the various regions in the density-temperature plane where one of the processes discussed above dominates. At low density and high temperature, κ has a constant value given by electron scattering. Opacity increases towards higher ρ and lower T due to free-free and bound-free absorptions. For $T < 10^4$ K opacity decreases drastically due to recombination of hydrogen, the main opacity source here is the H^- ion. At lower temperatures still, κ rises again

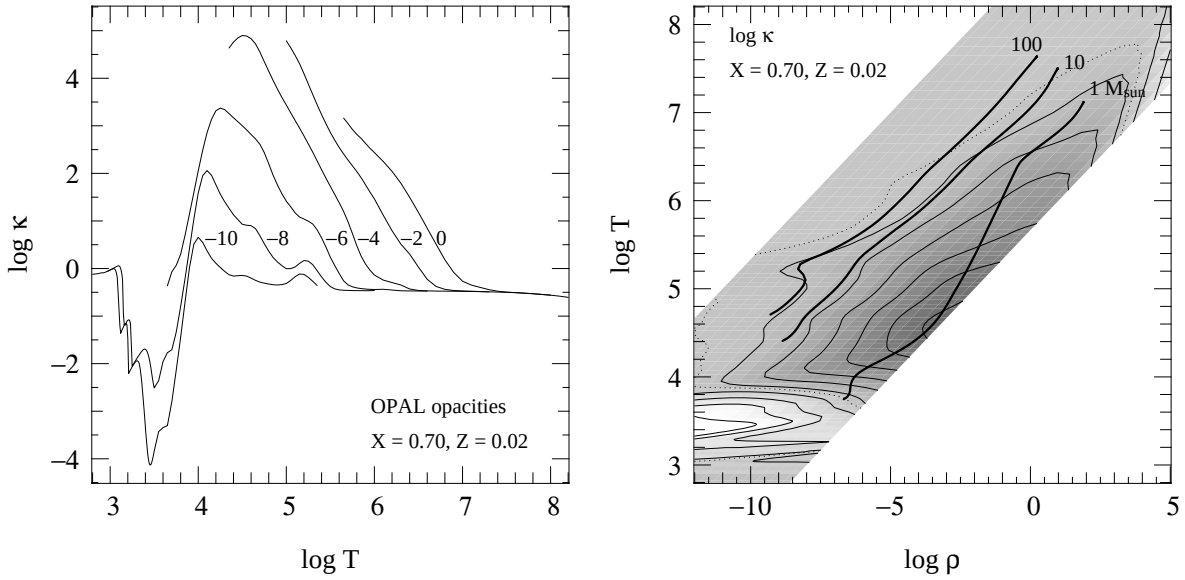

Figure 5.2. Rosseland mean opacities as a function of T and ρ, for a mixture of elements representative of solar abundances ($X = 0.7, Z = 0.02$), calculated by the OPAL project for high temperatures and by J. Ferguson for low temperatures ($\log T < 3.8$). The left panel shows curves of $\log\kappa$ (in cm^2/g) versus temperature for several values of the density, labelled by the value of $\log\rho$ (in g/cm^3). The right panel shows contour lines of constant $\log\kappa$ in the ρ-T plane, in steps of 1.0 between -4 and 5, over the region in temperature and density for which the radiative opacity has been calculated. The thick lines are detailed structure models for main-sequence stars of 1, 10 and 100 $M_\odot$, as in Fig. 3.4.

due to molecules and dust formation. Finally, at very high density the opacity is dominated by the conductivity of degenerate electrons and decreases strongly with increasing ρ (just visible in the upper right corner of Fig. 5.2). It should be clear that there is much more structure in the function $\kappa(\rho, T)$ than in the simple power-law approximations, such as the Kramers law. The many ridges and bumps show that the Kramers law is a rather poor approximation of the actual opacity.

For comparison, interior structure models for main-sequence stars of different masses are also shown. The opacity in the interior of a 1 $M_\odot$ star is dominated by free-free and bound-free absorption, and is very high (up to $10^5\,\mathrm{cm}^2/\mathrm{g}$) in the envelope, at temperatures between 10^4 and $10^5\,\mathrm{K}$. In the surface layers the opacity rapidly decreases due to the H^- opacity. More massive stars are located at lower densities than the Sun, and generally have much lower opacities in their envelopes. In the most massive stars the opacity is dominated by electron scattering, at low ρ and high T. However, even here one has to deal with additional opacity bumps, most prominently the one due to bound-free transitions of Fe at $\log T \approx 5.3$.

Note that the chemical composition, in particular the metallicity Z, can have a large effect on κ. This provides the most important influence of composition on stellar structure.

5.4 The Eddington luminosity

We have seen that radiative transport of energy inside a star requires a temperature gradient $\mathrm{d}T/\mathrm{d}r$, the magnitude of which is given by eq. (5.16). Since $P_\mathrm{rad} = \frac{1}{3}aT^4$, this means there is also a gradient in the radiation pressure:

$$\frac{\mathrm{d}P_\mathrm{rad}}{\mathrm{d}r} = -\frac{4}{3}aT^3\frac{\mathrm{d}T}{\mathrm{d}r} = -\frac{\kappa\rho}{4\pi c}\frac{l}{r^2}. \tag{5.36}$$

This radiation pressure gradient represents an outward force due to the net flux of photons outwards. Of course, for a star in hydrostatic equilibrium this outward radiation force must be smaller than the inward force of gravity, as given by the pressure gradient necessary for HE, eq. (2.12). In other words,

$$\left|\frac{\mathrm{d}P_\mathrm{rad}}{\mathrm{d}r}\right| < \left|\left(\frac{\mathrm{d}P}{\mathrm{d}r}\right)_\mathrm{HE}\right| \quad \Rightarrow \quad \frac{\kappa\rho}{4\pi c}\frac{l}{r^2} < \frac{Gm\rho}{r^2}.$$

This gives an upper limit to the local luminosity, which is known as the (local) *Eddington luminosity*,

$$l < \frac{4\pi cGm}{\kappa} = l_\mathrm{Edd}. \tag{5.37}$$

This is the maximum luminosity that can be carried by radiation, inside a star in hydrostatic equilibrium.

The inequality expressed by eq. (5.37) can be violated in the case of a very large heat flux (large l), which may result from intense nuclear burning, or in the case of a very high opacity κ. As we saw in Sec. 5.3, high opacities are encountered at relatively low temperatures, near the ionization temperature of hydrogen and helium (and for example in the outer layers of the Sun). In such cases hydrostatic equilibrium (eq. 2.13) and radiative equilibrium (eq. 5.17) cannot hold simultaneously. Therefore, if the star is to remain in HE, energy must be transported by a different means than radiative diffusion. This means of transport is *convection*, the collective motion of gas bubbles that carry heat and can distribute it efficiently. We shall consider convection in detail in Sec. 5.5. It will turn out that eq. (5.37) is a necessary, but not a sufficient condition for a region of a star to be stable against convection.

The surface layer of a star is always radiative, since it is from here that energy escapes the star in the form of photons. Applying eq. (5.37) at the surface of the star ($m = M$) we get

$$L < L_\mathrm{Edd} = \frac{4\pi cGM}{\kappa}, \tag{5.38}$$

where κ is the opacity in the photosphere. Violation of this condition now means violation of hydrostatic equilibrium: matter is accelerated away from the star by the photon pressure, giving rise to violent mass loss. The Eddington luminosity expressed by eq. (5.38) is a critical stellar luminosity that cannot be exceeded by a star in hydrostatic equilibrium. If we assume κ to be approximately constant (in very luminous main-sequence stars the opacity is dominated by electron scattering, so this is not a bad assumption) then $L_{\rm Edd}$ is only dependent on M. It can be expressed as follows

$$L_{\rm Edd} = 3.8 \times 10^4 \left(\frac{M}{M_\odot}\right)\left(\frac{0.34\,{\rm cm}^2/{\rm g}}{\kappa}\right) L_\odot. \tag{5.39}$$

The value of $0.34\,{\rm cm}^2/{\rm g}$ corresponds to the electron scattering opacity for $X = 0.7$.

Since $L_{\rm Edd}$ is proportional to M, while stars (at least on the main sequence) follow a mass-luminosity relation $L \propto M^x$ with $x > 1$ (Sec. 1.1.2), this implies that for stars of increasing mass L will at some point exceed $L_{\rm Edd}$. Hence, we can expect a *maximum mass* to exist for main-sequence stars. Note that the existence of a steep mass-luminosity relation (with $x \approx 3$) can be derived directly for stars in which energy transport occurs by radiation (see Exercise 5.3, and also Sec. 7.4), without having to assume anything about how energy is generated.

5.5 Convection

For radiative diffusion to transport energy outwards, a certain temperature gradient is needed, given by eq. (5.16) or eq. (5.17). The larger the luminosity that has to be carried, the larger the temperature gradient required. There is, however, an upper limit to the temperature gradient inside a star – if this limit is exceeded an instability in the gas sets in. This instability leads to cyclic macroscopic motions of the gas, known as *convection*. Convection can be regarded as a type of dynamical instability, although (as we shall see later in this section) it does not have disruptive consequences. In particular, it does not lead to an overall violation of hydrostatic equilibrium. Convection affects the structure of a star only as an efficient means of heat transport and as an efficient mixing mechanism.

In Sec. 5.4 we already derived an upper limit to the luminosity that can be transported by radiation. We will now derive a more stringent criterion for convection to occur, based on considerations of dynamical stability.

5.5.1 Criteria for stability against convection

So far we have assumed strict spherical symmetry in our description of stellar interiors, i.e. assuming all variables are constant on concentric spheres. In reality there will be small fluctuations, arising for example from the thermal motions of the gas particles. If these small perturbations do not grow they can safely be ignored. However, if the perturbations do grow they can give rise to macroscopic motions, such as convection. We therefore need to consider the *dynamical stability* of a layer inside a star against such perturbations.

Consider a mass element that, due to a small perturbation, is displaced upwards by a small distance as depicted in Fig. 5.3. At its original position (at radius r) the density and pressure are ρ_1 and P_1, and at its new position ($r + \Delta r$) the ambient density and pressure are ρ_2 and P_2. Since pressure decreases outwards, $P_2 < P_1$ and the gas element will expand to restore pressure equilibrium with its surroundings. Hence the pressure of the gas element at position 2 is $P_e = P_2$, but its new density after expansion ρ_e is not necessarily equal to ρ_2. If $\rho_e > \rho_2$, the gas element will experience a net buoyancy force downwards (by Archimedes' law), which pushes it back towards its original position. Then the small perturbation is quenched, and the situation is stable. On the other hand, if $\rho_e < \rho_2$ then there is a net buoyancy force upwards and we have an *unstable* situation that leads to convection.

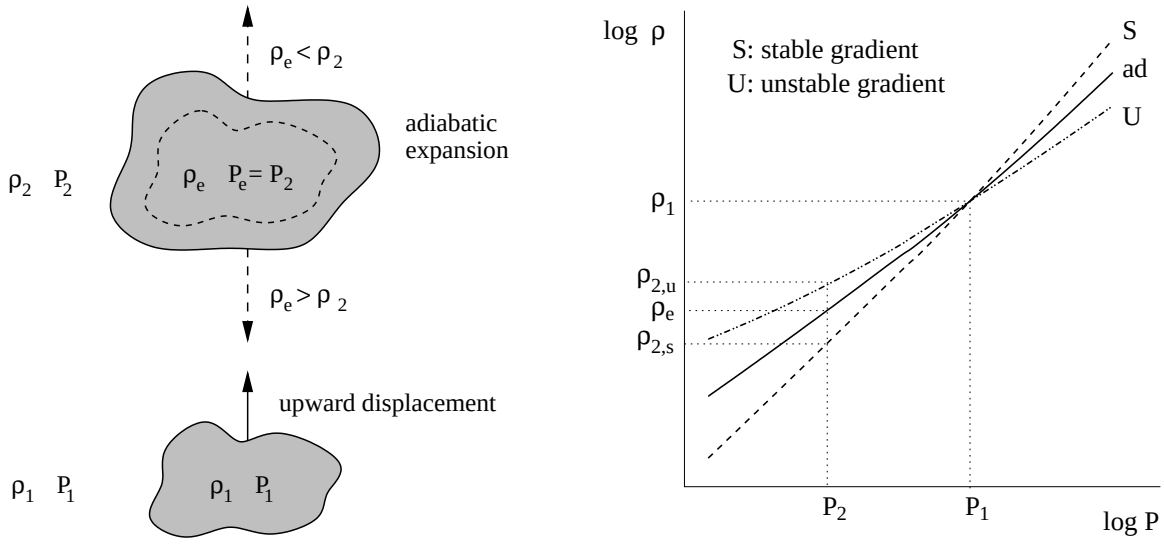

Figure 5.3. Schematic illustration of the Schwarzschild criterion for stability against convection. A gas element is perturbed and displaced upwards from position 1 to position 2, where it expands adiabatically to maintain pressure equilibrium with its surroundings. If its density is larger than the ambient density, it will sink back to its original position. If its density is smaller, however, buoyancy forces will accelerate it upwards: convection occurs. On the right the situation is shown in a density-pressure diagram. A layer is stable against convection if the density varies more steeply with pressure than for an adiabatic change.

The expansion of the gas element as it rises over Δr occurs on the local dynamical timescale (i.e. with the speed of sound), which is typically much shorter than the local timescale for heat exchange, at least in the deep interior of the star. The displacement and expansion of the gas element will therefore be very close to adiabatic. We have seen in Sec. 3.4 that the adiabatic exponent $\gamma_{\rm ad}$ defined by eq. (3.56) describes the logarithmic response of the pressure to an adiabatic change in the density. Writing as $\delta\rho_e$ and δP_e the changes in the density and pressure of the element when it is displaced over a small distance Δr, we therefore have

$$\frac{\delta P_e}{P_e} = \gamma_{\rm ad} \frac{\delta\rho_e}{\rho_e}. \tag{5.40}$$

Here δP_e is determined by the pressure gradient $\mathrm{d}P/\mathrm{d}r$ inside the star because $P_e = P_2$, i.e. $\delta P_e = P_2 - P_1 = (\mathrm{d}P/\mathrm{d}r)\,\Delta r$. Therefore the change in density $\delta\rho_e$ follows from eq. (5.40)

$$\delta\rho_e = \frac{\rho_e}{P_e} \frac{1}{\gamma_{\rm ad}} \frac{\mathrm{d}P}{\mathrm{d}r} \Delta r. \tag{5.41}$$

We can write $\rho_e = \rho_1 + \delta\rho_e$ and $\rho_2 = \rho_1 + (\mathrm{d}\rho/\mathrm{d}r)\,\Delta r$, where $\mathrm{d}\rho/\mathrm{d}r$ is the density gradient inside the star. We can then express the criterion for stability against convection, $\rho_e > \rho_2$, as

$$\delta\rho_e > \frac{\mathrm{d}\rho}{\mathrm{d}r} \Delta r, \tag{5.42}$$

which combined with eq. (5.41) yields an upper limit to the density gradient for which a layer inside the star is stable against convection,

$$\frac{1}{\rho}\frac{\mathrm{d}\rho}{\mathrm{d}r} < \frac{1}{P}\frac{\mathrm{d}P}{\mathrm{d}r}\frac{1}{\gamma_{\rm ad}}, \tag{5.43}$$

where we have replaced P_e and ρ_e by P and ρ, since the perturbations are assumed to be very small. Remember, however, that both $\mathrm{d}\rho/\mathrm{d}r$ and $\mathrm{d}P/\mathrm{d}r$ are negative. Therefore, in absolute value the sign

of eq. (5.43) reverses, which means that the density gradient must be *steeper* than a critical value, determined by $\gamma_{\rm ad}$. If we divide (5.43) by dP/dr we obtain the general criterion for stability against convection, which is depicted on the right-hand side in Fig. 5.3,

$$\frac{\mathrm{d}\log\rho}{\mathrm{d}\log P} > \frac{1}{\gamma_{\rm ad}}. \tag{5.44}$$

If condition (5.44) is violated then convective motions will develop. Gas bubbles that, due to a small perturbation, are slightly hotter than their surroundings will move up, transporting their heat content upwards until they are dissolved. Other bubbles may be slightly cooler than their environment, these will move down and have a smaller heat content than their surroundings. When these bubbles finally dissolve, they absorb heat from their surroundings. Therefore, both the upward and downward moving convective bubbles effectively transport heat in the upward direction. Hence there is a *net upward heat flux*, even though there is no net mass flux, since upward and downward moving bubbles carry equal amounts of mass. This is the principle behind convective heat transport.

The Schwarzschild and Ledoux criteria

The stability criterion (5.44) is not of much practical use, because it involves computation of a density gradient which is not part of the stellar structure equations. We would rather have a criterion for the temperature gradient, because this also appears in the equation for radiative transport. We can rewrite eq. (5.44) in terms of temperature by using the equation of state. We write the equation of state in its general, differential form (eq. 3.48) but now also take into account a possible variation in composition. If we characterize the composition by the mean molecular weight μ then $P = P(\rho, T, \mu)$ and we can write

$$\frac{\mathrm{d}P}{P} = \chi_T \frac{\mathrm{d}T}{T} + \chi_\rho \frac{\mathrm{d}\rho}{\rho} + \chi_\mu \frac{\mathrm{d}\mu}{\mu}, \tag{5.45}$$

with χ_T and χ_ρ defined by eqs. (3.49) and (3.50), and χ_μ is defined as

$$\chi_\mu = \left(\frac{\partial \log P}{\partial \log \mu}\right)_{\rho,T}. \tag{5.46}$$

For an ideal gas $\chi_\mu = -1$. With the help of eq. (5.45) we can write the variation of density with pressure through the star as

$$\frac{\mathrm{d}\log\rho}{\mathrm{d}\log P} = \frac{1}{\chi_\rho}\left(1 - \chi_T \frac{\mathrm{d}\log T}{\mathrm{d}\log P} - \chi_\mu \frac{\mathrm{d}\log\mu}{\mathrm{d}\log P}\right) = \frac{1}{\chi_\rho}(1 - \chi_T\nabla - \chi_\mu\nabla_\mu). \tag{5.47}$$

Here we have introduced, by analogy with eq. (5.18), the symbols $\nabla \equiv \mathrm{d}\log T/\mathrm{d}\log P$ and $\nabla_\mu \equiv \mathrm{d}\log\mu/\mathrm{d}\log P$. These quantities represent the actual gradients of temperature and of mean molecular weight through the star, regarding P as the variable that measures depth. In the displaced gas element the composition does not change, and from eq. (3.63) we can write

$$\frac{1}{\gamma_{\rm ad}} = \frac{1}{\chi_\rho}(1 - \chi_T\nabla_{\rm ad}),$$

so that the stability criterion (5.44) becomes

$$\nabla < \nabla_{\rm ad} - \frac{\chi_\mu}{\chi_T}\nabla_\mu. \tag{5.48}$$

If all the energy is transported by radiation then $\nabla = \nabla_{\rm rad}$ as given by eq. (5.18). Hence we can replace ∇ by $\nabla_{\rm rad}$ in eq. (5.48) and thus arrive at the *Ledoux criterion* which states that a layer is stable against convection if

$$\boxed{\nabla_{\rm rad} < \nabla_{\rm ad} - \frac{\chi_\mu}{\chi_T}\nabla_\mu} \qquad \text{(Ledoux)} \tag{5.49}$$

In chemically homogeneous layers $\nabla_\mu = 0$ and eq. (5.49) reduces to the simple *Schwarzschild criterion* for stability against convection[1]

$$\boxed{\nabla_{\rm rad} < \nabla_{\rm ad}} \qquad \text{(Schwarzschild)} \tag{5.50}$$

N.B. Note the difference in meaning of the various ∇ symbols appearing in the above criteria: $\nabla_{\rm rad}$ and ∇_μ represent a *spatial* gradient of temperature and mean molecular weight, respectively. On the other hand, $\nabla_{\rm ad}$ represents the adiabatic temperature variation in a specific gas element undergoing a change in pressure.

For an ideal gas ($\chi_T = 1, \chi_\mu = -1$) the Ledoux criterion reduces to

$$\nabla_{\rm rad} < \nabla_{\rm ad} + \nabla_\mu. \tag{5.51}$$

The mean molecular weight normally increases inwards, because in deeper layers nuclear reactions have produced more and more heavy elements. Therefore normally $\nabla_\mu \geq 0$, so that according to the Ledoux criterion a composition gradient has a stabilizing effect. This is plausible because an upwards displaced element will then have a higher μ than its surroundings, so that even when it is hotter than its new environment (which would make it unstable according to the Schwarzschild criterion) it has a higher density and the buoyancy force will push it back down.

Occurrence of convection

According to the Schwarzschild criterion, we can expect convection to occur if

$$\nabla_{\rm rad} = \frac{3}{16\pi acG}\frac{P}{T^4}\frac{\kappa l}{m} > \nabla_{\rm ad}. \tag{5.52}$$

This requires one of following:

- A large value of κ, that is, convection occurs in opaque regions of a star. Examples are the outer envelope of the Sun (see Fig. 5.2) and of other cool stars, because opacity increases with decreasing temperature. Since low-mass stars are cooler than high-mass stars, we may expect low-mass stars to have convective envelopes.

- A large value of l/m, i.e. regions with a large energy flux. We note that towards the centre of a star $l/m \approx \epsilon_{\rm nuc}$ by eq. (5.4), so that stars with nuclear energy production that is strongly peaked towards the centre can be expected to have convective cores. We shall see that this is the case for relatively massive stars.

[1] We can relate the convection criterion to the Eddington limit derived in Sec. 5.4. By writing $\nabla_{\rm rad}$ in terms of l, $l_{\rm Edd}$ (defined in eq. 5.37) and $P_{\rm rad} = (1-\beta)P$ we can rewrite the Schwarzschild criterion for stability as

$$l < 4(1-\beta)\nabla_{\rm ad}\, l_{\rm Edd}$$

(see Exercise 5.6). For $\beta > 0$ and $\nabla_{\rm ad} > 0.25$ we see that convection already sets in before the Eddington limit is reached.

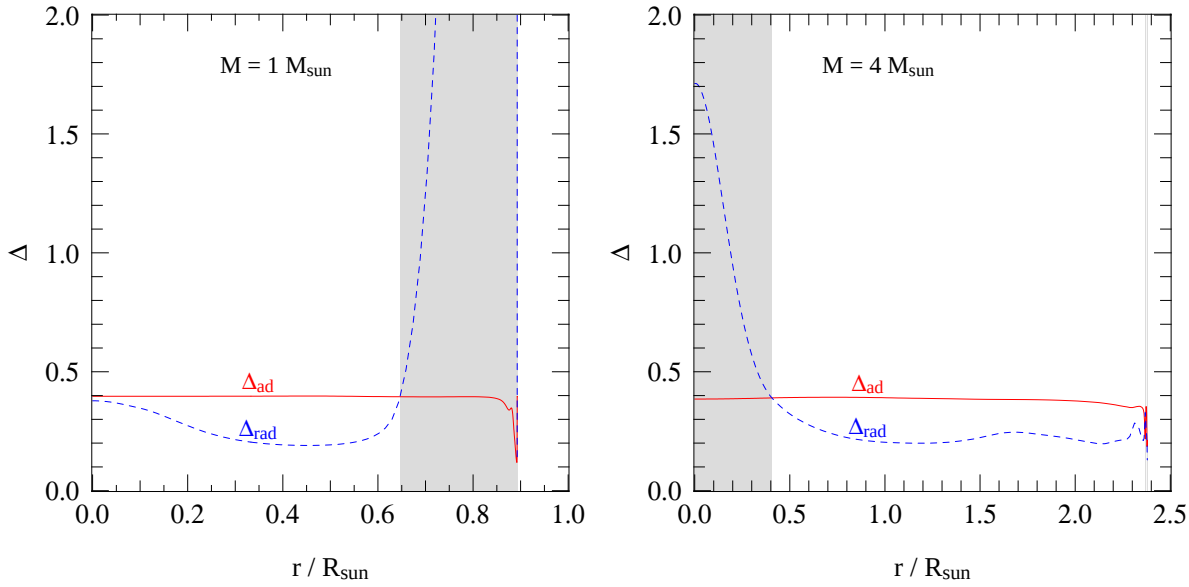

Figure 5.4. The variation of $\nabla_{\rm ad}$ (red, solid line) and $\nabla_{\rm rad}$ (blue, dashed line) with radius in two detailed stellar models of $1\,M_\odot$ and $4\,M_\odot$ at the start of the main sequence. The solar-mass model has a very large opacity in its outer layers, resulting in a large value of $\nabla_{\rm rad}$ which gives rise to a convective envelope where $\nabla_{\rm rad} > \nabla_{\rm ad}$ (indicated by gray shading). On the other hand, the $4\,M_\odot$ model has a hotter outer envelope with lower opacity so that $\nabla_{\rm rad}$ stays small. The large energy generation rate in the centre now results in a large $\nabla_{\rm rad}$ and a convective core extending over the inner $0.4\,R_\odot$. In both models $\nabla_{\rm ad} \approx 0.4$ since the conditions are close to an ideal gas. In the surface ionization zones, however, $\nabla_{\rm ad} < 0.4$ and a thin convective layer appears in the $4\,M_\odot$ model.

- A small value of $\nabla_{\rm ad}$, which as we have seen in Sec. 3.5 occurs in partial ionization zones at relatively low temperatures. Therefore, even if the opacity is not very large, the surface layers of a star may be unstable to convection. It turns out that stars of all masses have shallow surface convection zones at temperatures where hydrogen and helium are partially ionized.

These effects are illustrated in Fig. 5.4.

5.5.2 Convective energy transport

We still have to address the question how much energy can be transported by convection and, related to this, what is the actual temperature gradient ∇ inside a convective region. To answer these questions properly requires a detailed theory of convection, which to date remains a very difficult problem in astrophysics that is still unsolved. Even though convection can be simulated numerically, this requires solving the equations of hydrodynamics in three dimensions over a huge range of length scales and time scales, and of pressures, densities and temperatures. Such simulations are therefore very time-consuming and still limited in scope, and cannot be applied in stellar evolution calculations. We have to resort to a very simple one-dimensional 'theory' that is based on rough estimates, and is known as the *mixing length theory* (MLT).

In the MLT one approximates the complex convective motions by blobs of gas that travel up or down over a radial distance $\ell_{\rm m}$ (the mixing length), after which they dissolve in their surroundings and lose their identity. As the blob dissolves it releases its excess heat to its surroundings (or, in the case of a downward moving blob, it absorbs its heat deficit from its surroundings). The mixing length $\ell_{\rm m}$ is an unknown free parameter in this very schematic model. One presumes that $\ell_{\rm m}$ is of the order

of the local pressure scale height, which is the radial distance over which the pressure changes by an e-folding factor,

$$H_P = \left| \frac{\mathrm{d}r}{\mathrm{d}\ln P} \right| = \frac{P}{\rho g}. \tag{5.53}$$

The last equality holds for a star in hydrostatic equilibrium. The assumption that $\ell_\mathrm{m} \sim H_P$ is not unreasonable considering that a rising gas blob will expand. Supposing that in a convective region in a star, about half of a spherical surface area is covered by rising blobs and the other half by sinking blobs, the expanding rising blobs will start covering most of the surface area after rising over one or two pressure scale heights.

The convective energy flux

Within the framework of MLT we can calculate the convective energy flux, and the corresponding temperature gradient required to carry this flux, as follows. After rising over a radial distance ℓ_m the temperature difference between the gas element (e) and its surroundings (s) is

$$\Delta T = T_\mathrm{e} - T_\mathrm{s} = \left[\left(\frac{\mathrm{d}T}{\mathrm{d}r} \right)_\mathrm{e} - \frac{\mathrm{d}T}{\mathrm{d}r} \right] \ell_\mathrm{m} = \Delta \left(\frac{\mathrm{d}T}{\mathrm{d}r} \right) \ell_\mathrm{m}.$$

Here $\mathrm{d}T/\mathrm{d}r$ is the ambient temperature gradient, $(\mathrm{d}T/\mathrm{d}r)_e$ is the variation of temperature with radius that the element experiences as it rises and expands adiabatically, and $\Delta(\mathrm{d}T/\mathrm{d}r)$ is the difference between these two. We can write ΔT in terms of ∇ and ∇_ad by noting that

$$\frac{\mathrm{d}T}{\mathrm{d}r} = T \, \frac{\mathrm{d}\ln T}{\mathrm{d}r} = T \, \frac{\mathrm{d}\ln T}{\mathrm{d}\ln P} \, \frac{\mathrm{d}\ln P}{\mathrm{d}r} = -\frac{T}{H_P} \, \nabla \qquad \text{and} \qquad \left(\frac{\mathrm{d}T}{\mathrm{d}r} \right)_e = -\frac{T}{H_P} \, \nabla_\mathrm{ad},$$

noting that the '$-$' sign appears because $\mathrm{d}P/\mathrm{d}r < 0$ in eq. (5.53). Hence

$$\Delta T = T \, \frac{\ell_\mathrm{m}}{H_P} \, (\nabla - \nabla_\mathrm{ad}). \tag{5.54}$$

The excess of internal energy of the gas element compared to its surroundings is $\Delta u = c_P \Delta T$ per unit mass. If the convective blobs move with an average velocity v_c, then the energy flux carried by the convective gas elements is

$$F_\mathrm{conv} = v_\mathrm{c} \, \rho \Delta u = v_\mathrm{c} \, \rho c_P \Delta T \tag{5.55}$$

We therefore need an estimate of the average convective velocity. If the difference in density between a gas element and its surroundings is $\Delta\rho$, then the buoyancy force will give an acceleration

$$a = -g \, \frac{\Delta\rho}{\rho} \approx g \, \frac{\Delta T}{T},$$

where the last equality is exact for an ideal gas for which $P \propto \rho T$ and $\Delta P = 0$. The blob is accelerated over a distance ℓ_m, i.e. for a time t given by $\ell_\mathrm{m} = \frac{1}{2} a t^2$. Therefore its average velocity is $v_\mathrm{c} \approx \ell_\mathrm{m}/t = \sqrt{\frac{1}{2} \ell_\mathrm{m} a}$, that is

$$v_\mathrm{c} \approx \sqrt{\tfrac{1}{2} \ell_\mathrm{m} g \frac{\Delta T}{T}} \approx \sqrt{\frac{{\ell_\mathrm{m}}^2 g}{2 H_P} \, (\nabla - \nabla_\mathrm{ad})}. \tag{5.56}$$

Combining this with eq. (5.55) gives

$$F_\mathrm{conv} = \rho c_P T \left(\frac{\ell_\mathrm{m}}{H_P} \right)^2 \sqrt{\tfrac{1}{2} g H_P} \, (\nabla - \nabla_\mathrm{ad})^{3/2}. \tag{5.57}$$

The above two equations relate the convective velocity and the convective energy flux to the so-called *superadiabaticity* $\nabla - \nabla_\mathrm{ad}$, the degree to which the actual temperature gradient ∇ exceeds the adiabatic value.

Estimate of the convective temperature gradient

Which value of $\nabla - \nabla_{\rm ad}$ is required to carry the whole energy flux of a star by convection, i.e. $F_{\rm conv} = l/4\pi r^2$? To make a rough estimate, we take typical values for the interior making use of the virial theorem and assuming an ideal gas:

$$\rho \approx \bar{\rho} = \frac{3M}{4\pi R^3} \qquad T \approx \bar{T} \sim \frac{\mu}{\mathcal{R}} \frac{GM}{R} \qquad c_P = \frac{5}{2}\frac{\mathcal{R}}{\mu} \qquad \sqrt{gH_P} = \sqrt{\frac{P}{\rho}} = \sqrt{\frac{\mathcal{R}}{\mu}T} \sim \sqrt{\frac{GM}{R}}$$

noting that the last expression is also approximately equal to the average speed of sound $\upsilon_{\rm s}$ in the interior. We then obtain, neglecting factors of order unity,

$$F_{\rm conv} \sim \frac{M}{R^3}\left(\frac{GM}{R}\right)^{3/2} (\nabla - \nabla_{\rm ad})^{3/2}. \tag{5.58}$$

If we substitute $F_{\rm conv} = l/4\pi r^2 \sim L/R^2$ then we can rewrite the above to

$$\nabla - \nabla_{\rm ad} \sim \left(\frac{LR}{M}\right)^{2/3} \frac{R}{GM} \tag{5.59}$$

Putting in typical numbers, i.e. solar luminosity, mass and radius, we obtain the following rough estimate for the superadiabaticity in the deep interior of a star like the Sun

$$\nabla - \nabla_{\rm ad} \sim 10^{-8}$$

Convection is so efficient at transporting energy that only a tiny superadiabaticity is required. This means that $F_{\rm conv} \gg F_{\rm rad}$ in convective regions. A more accurate estimate yields $\nabla - \nabla_{\rm ad} \sim 10^{-5} - 10^{-7}$, which is still a very small number. We can conclude that in the deep stellar interior the actual temperature stratification is nearly adiabatic, and independent of the details of the theory. Therefore a detailed theory of convection is not needed for energy transport by convection and we can simply take

$$\frac{{\rm d}T}{{\rm d}m} = -\frac{Gm}{4\pi r^4}\frac{T}{P}\nabla \qquad \text{with} \qquad \nabla = \nabla_{\rm ad}. \tag{5.60}$$

However in the outermost layers the situation is different, because $\rho \ll \bar{\rho}$ and $T \ll \bar{T}$. Therefore $F_{\rm conv}$ is much smaller and the superadiabaticity becomes substantial ($\nabla > \nabla_{\rm ad}$). The actual temperature gradient then depends on the details of the convection theory. Within the context of MLT, the T-gradient depends on the assumed value of $\alpha_{\rm m} = \ell_{\rm m}/H_P$. In practice one often calibrates detailed models computed with different values of $\alpha_{\rm m}$ to the radius of the Sun and of other stars with well-measured radii. The result of this procedure is that the best match is obtained for $\alpha_{\rm m} \approx 1.5$–$2$.

As the surface is approached, convection becomes very inefficient at transporting energy. Then $F_{\rm conv} \ll F_{\rm rad}$ so that radiation effectively transports all the energy, and $\nabla \approx \nabla_{\rm rad}$ despite convection taking place. These effects are shown in Fig. 5.5 for a detailed solar model.

5.5.3 Convective mixing

Besides being an efficient means of transporting energy, convection is also a very efficient *mixing mechanism*. We can see this by considering the average velocity of convective cells, eq. (5.56), and taking $\ell_{\rm m} \approx H_P$ and $\sqrt{gH_P} \approx \upsilon_{\rm s}$, so that

$$\upsilon_{\rm c} \approx \upsilon_{\rm s}\sqrt{\nabla - \nabla_{\rm ad}}. \tag{5.61}$$

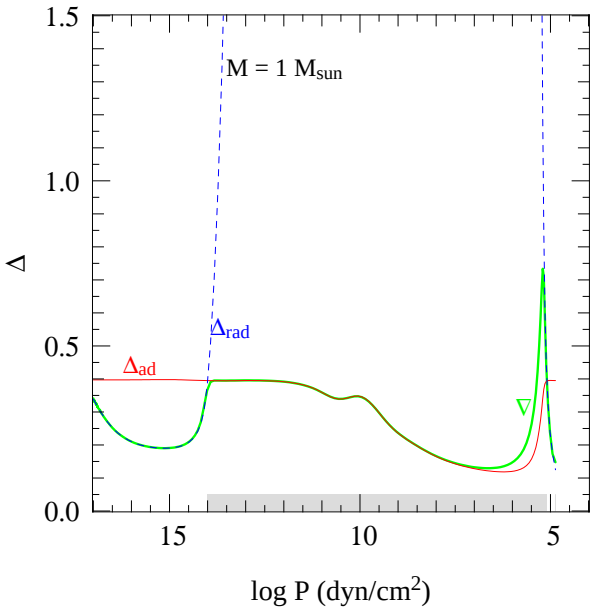

Figure 5.5. The variation of $\nabla_{\rm ad}$ (red, solid line) and $\nabla_{\rm rad}$ (blue, dashed line) in the same detailed model of 1 $M_\odot$ as shown in Fig. 5.4, but now plotted against $\log P$ rather than radius to focus on the outermost layers (where the pressure gradient is very large). The thick green line shows the actual temperature gradient ∇. The partial ionization zones are clearly visible as depressions in $\nabla_{\rm ad}$ (compare to Fig. 3.5b). The convection zone stretches from $\log P \approx 14$ to 5 (indicated by a gray bar along the bottom). In the deep interior (for $\log P > 8$) convection is very efficient and $\nabla = \nabla_{\rm ad}$. Higher up, at lower pressures, convection becomes less and less efficient at transporting energy and requires a larger T-gradient, $\nabla > \nabla_{\rm ad}$. In the very outer part of the convection zone convection is very inefficient and $\nabla \approx \nabla_{\rm rad}$.

Because $\nabla - \nabla_{\rm ad}$ is only of the order 10^{-6} in the deep interior, typical convective velocities are strongly subsonic, by a factor $\sim 10^{-3}$, except in the very outer layers where $\nabla - \nabla_{\rm ad}$ is substantial. This is the main reason why convection has no disruptive effects, and overall hydrostatic equilibrium can be maintained in the presence of convection.

By substituting into eq. (5.61) rough estimates for the interior of a star, i.e. $v_{\rm s} \sim \sqrt{GM/R}$ and eq. (5.59) for $\nabla - \nabla_{\rm ad}$, we obtain $v_{\rm c} \sim (LR/M)^{1/3} \approx 5 \times 10^3$ cm/s for a star like the Sun. These velocities are large enough to mix a convective region on a small timescale. We can estimate the timescale on which a region of radial size $d = qR$ is mixed as $\tau_{\rm mix} \approx d/v_{\rm c} \sim q(R^2 M/L)^{1/3}$, which is $\sim q \times 10^7$ sec for solar values. Depending on the fractional extent q of a convective region, the convective mixing timescale is of the order of weeks to months. Hence $\tau_{\rm mix} \ll \tau_{\rm KH} \ll \tau_{\rm nuc}$, so that over a thermal timescale, and certainly over a nuclear timescale, a convective region inside a star will be mixed homogeneously. (Note that convective mixing remains very efficient in the outer layers of a star, even though convection becomes inefficient at transporting energy.)

This has important consequences for stellar evolution, which we will encounter in future chapters. Briefly, the large efficiency of convective mixing means that:

- A star in which nuclear burning occurs in a *convective core* will homogenize the region inside the core by transporting burning ashes (e.g. helium) outwards and fuel (e.g. hydrogen) inwards. Such a star therefore has a larger fuel supply and can extend its lifetime compared to the hypothetical case that convection would not occur.

- A star with a deep *convective envelope*, such that it extends into regions where nuclear burning has taken place, will mix the burning products outwards towards the surface. This process

(often called ‘dredge-up’), which happens when stars become red giants, can therefore modify the surface composition, and in such a star measurements of the surface abundances provide a window into nuclear processes that have taken place deep inside the star.

Composition changes inside a star will be discussed in the next chapter.

5.5.4 Convective overshooting

To determine the extent of a region that is mixed by convection, we need to look more closely at what happens at the boundary of a convective zone. According to the Schwarzschild criterion derived in Sec. 5.5.1, in a chemically homogeneous layer this boundary is located at the surface where $\nabla_{\rm rad} = \nabla_{\rm ad}$. At this point the acceleration due to the buoyancy force, $a \approx g(\nabla - \nabla_{\rm ad})$, vanishes. Just outside this boundary, the acceleration changes sign and a convective bubble will be strongly braked – even more so when the non-mixed material outside the convective zone has a lower μ and hence a lower density. However, the convective eddies have (on average) a non-zero velocity when they cross the Schwarzschild boundary, and will *overshoot* by some distance due to their inertia. A simple estimate of this overshooting distance shows that it should be much smaller than a pressure scale height, so that the Schwarzschild criterion should determine the convective boundary quite accurately. However the convective elements also carry some heat and mix with their surroundings, so that both $|\nabla - \nabla_{\rm ad}|$ and the μ-gradient decrease. Thus also the effective buoyancy force that brakes the elements decreases, and a positive feedback loop can develop that causes overshooting elements to penetrate further and further. This is a highly non-linear effect, and as a result the actual overshooting distance is very uncertain and could be substantial.

Convective overshooting introduces a large uncertainty in the extent of mixed regions, with important consequences for stellar evolution. A convectively mixed core that is substantially larger will generate a larger fuel supply for nuclear burning, and thus affects both the hydrogen-burning lifetime and the further evolution of a star. In stellar evolution calculations one usually parametrizes the effect of overshooting by assuming that the distance $d_{\rm ov}$ by which convective elements penetrate beyond the Schwarzschild boundary is a fixed fraction of the local pressure scale height, $d_{\rm ov} = \alpha_{\rm ov} H_P$. Here $\alpha_{\rm ov}$ is a free parameter, that can be calibrated against observations (see Chapter 9).

Suggestions for further reading

The contents of this chapter are also covered by Chapters 3, 5 and 8 of Maeder, by Chapters 4, 5, 7 and 17 of Kippenhahn and by Chapters 4 and 5 of Hansen.

Exercises

5.1 Radiation transport

The most important way to transport energy form the interior of the star to the surface is by radiation, i.e. photons traveling from the center to the surface.

(a) How long does it typically take for a photon to travel from the center of the Sun to the surface? [Hint: estimate the mean free path of a photon in the central regions of the Sun.] How does this relate to the thermal timescale of the Sun?

(b) Estimate a typical value for the temperature gradient $\mathrm{d}T/\mathrm{d}r$. Use it to show that the difference in temperature ΔT between to surfaces in the solar interior one photon mean free path $\ell_{\rm ph}$ apart is

$$\Delta T = \ell_{\rm ph} \frac{\mathrm{d}T}{\mathrm{d}r} \approx 2 \times 10^{-4}\,\mathrm{K}.$$

In other words the anisotropy of radiation in the stellar interior is very small. This is why radiation in the solar interior is close to that of a black body.

(c) Verify that a gas element in the solar interior, which radiates as a black body, emits $\approx 6 \times 10^{23}\,\mathrm{erg\,cm^{-2}\,s^{-1}}$.

If the radiation field would be exactly isotropic, then the same amount of energy would radiated into this gas element by the surroundings and so there would be no net flux.

(d) Show that the minute deviation from isotropy between two surfaces in the solar interior one photon mean free path apart at $r \sim R_\odot/10$ and $T \sim 10^7$ K, is sufficient for the transfer of energy that results in the luminosity of the Sun.

(e) Why does the diffusion approximation for radiation transport break down when the surface (photosphere) of a star is approached?

5.2 Opacity

(a) Identify the various processes contributing to the opacity as shown in Fig. 5.2, and the T and ρ ranges where they are important.

(b) Compare the opacity curve for $\log\rho = -6$ in the left panel of Fig. 5.2 to the approximations given in Sec. 5.3.1 for (1) electron scattering, (2) free-free absorption, (3) bound-free absorption and (4) the H^- ion. How well do these approximations fit the realistic opacity curve?

(c) Calculate (up to an order of magnitude) the photon mean free path in a star of 1 $M_\odot$ at radii where the temperature is 10^7 K, 10^5 K and 10^4 K, using the right panel of Fig. 5.2.

(d) Suppose that the frequency-dependent opacity coefficient has the form $\kappa_\nu = \kappa_0 \nu^{-\alpha}$. Show that the Rosseland mean opacity depends on the temperature as $\kappa \propto T^{-\alpha}$.

5.3 Mass-luminosity relation for stars in radiative equilibrium

Without solving the stellar structure equations, we can already derive useful scaling relations. In this question you will use the equation for radiative energy transport with the equation for hydrostatic equilibrium to derive a scaling relation between the mass and the luminosity of a star.

(a) Derive how the central temperature, T_c, scales with the mass, M, radius, R, and luminosity, L, for a star in which the energy transport is by radiation. To do this, use the stellar structure equation (5.16) for the temperature gradient in radiative equilibrium. Assume that $r \sim R$ and that the temperature is proportional to T_c, $l \sim L$ and estimating $\mathrm{d}T/\mathrm{d}r \sim -T_c/R$.

(b) Derive how T_c scales with M and R, using the hydrostatic equilibrium equation, and assuming that the ideal gas law holds.

(c) Combine the results obtained in (a) and (b), to derive how L scales with M and R for a star whose energy transport is radiative.

You have arrived at a mass-luminosity relation without assuming anything about how the energy is *produced*, only about how it is *transported* (by radiation). It shows that the luminosity of a star is *not* determined by the rate of energy production in the centre, but by how fast it can be transported to the surface!

(d) Compare your answer to the relation between M and L which you derived from observations (Exercise 1.3). Why does the derived power-law relation start to deviate from observations for low mass stars? Why does it deviate for high mass stars?

5.4 Conceptual questions: convection

(a) Why does convection lead to a net heat flux upwards, even though there is no net mass flux (upwards and downwards bubbles carry equal amounts of mass)?

(b) Explain the Schwarzschild criterion

$$\left(\frac{d\ln T}{d\ln P}\right)_{\rm rad} > \left(\frac{d\ln T}{d\ln P}\right)_{\rm ad}$$

in simple physical terms (using Archimedes law) by drawing a schematic picture . Consider both cases $\nabla_{\rm rad} > \nabla_{\rm ad}$ and $\nabla_{\rm rad} < \nabla_{\rm ad}$. Which case leads to convection?

(c) What is meant by the *superadiabaticity* of a convective region? How is it related to the convective energy flux (qualitatively)? Why is it very small in the interior of a star, but can be large near the surface?

5.5 Applying Schwarzschild's criterion

(a) Low-mass stars, like the Sun, have convective envelopes. The fraction of the mass that is convective increases with decreasing mass. A 0.1 $M_\odot$ star is completely convective. Can you qualitatively explain why?

(b) In contrast higher-mass stars have radiative envelopes and convective cores, for reasons we will discuss in the coming lectures. Determine if the energy transport is convective or radiative at two different locations ($r = 0.242R_\odot$ and $r = 0.670R_\odot$) in a $5M_\odot$ main sequence star. Use the data of a 5 $M_\odot$ model in the table below. You may neglect the radiation pressure and assume that the mean molecular weight $\mu = 0.7$.

$r/R_\odot$	$m/M_\odot$	$L_r/L_\odot$	T [K]	ρ [g cm^{-3}]	κ [g^{-1} cm^2]
0.242	0.199	3.40×10^2	2.52×10^7	18.77	0.435
0.670	2.487	5.28×10^2	1.45×10^7	6.91	0.585

5.6 The Eddington luminosity

The Eddington luminosity is the maximum luminosity a star (with radiative energy transport) can have, where radiation force equals gravity.

(a) Show that

$$l_{\rm max} = \frac{4\pi cGm}{\kappa}.$$

(b) Consider a star with a uniform opacity κ and of uniform parameter $1-\beta = P_{\rm rad}/P$. Show that $L/L_{\rm Edd} = 1-\beta$ for such a star.

(c) Show that the Schwarzschild criterion for stability against convection $\nabla_{\rm rad} < \nabla_{\rm ad}$ can be rewritten as:

$$\frac{l}{l_{\rm max}} < 4\frac{P_{\rm rad}}{P}\nabla_{\rm ad}$$

(d) Consider again the star of question (b). By assuming that it has a convective core, and no nuclear energy generation outside the core, show that the mass fraction of this core is given by

$$\frac{M_{\rm core}}{M} = \frac{1}{4\nabla_{\rm ad}}.$$

Chapter 6

Nuclear processes in stars

For a star in thermal equilibrium, an internal energy source is required to balance the radiative energy loss from the surface. This energy source is provided by *nuclear reactions* that take place in the deep interior, where the temperature and density are sufficiently high. In ordinary stars, where the ideal-gas law holds, this stellar nuclear reactor is very stable: the rate of nuclear reactions adapts itself to produce exactly the amount of energy that the star radiates away from its surface. Nuclear reactions do not determine the luminosity of the star – this is set by how fast the energy can be transported, i.e. by the opacity of the stellar gas – but they do determine for how long the star is able to sustain its luminosity. In stars composed of degenerate gas, on the other hand, nuclear reactions are unstable and may give rise to flashes or even explosions.

Apart from energy generation, another important effect of nuclear reactions is that they change the composition by transmutations of chemical elements into other, usually heavier, elements. In this way stars produces all the elements in the Universe heavier than helium – a process called *stellar nucleosynthesis*.

6.1 Basic nuclear properties

Consider a reaction whereby a nucleus X reacts with a particle a, producing a nucleus Y and a particle b. This can be denoted as

$$X + a \rightarrow Y + b \qquad \text{or} \qquad X(a,b)Y \quad . \tag{6.1}$$

The particle a is generally another nucleus, while the particle b could also be a nucleus, a γ-photon or perhaps another kind of particle. Some reactions produce more than two particles (e.g. when a weak interaction is involved, an electron and anti-neutrino can be produced in addition to nucleus Y), but the general principles discussed here also apply to reactions involving different numbers of nuclei. Each nucleus is characterized by two integers, the charge Z_i (representing the number of protons in the nucleus) and the baryon number or mass number A_i (equal to the total number of protons plus neutrons). Charges and baryon numbers must be conserved during a reaction, i.e. for the example above:

$$Z_X + Z_a = Z_Y + Z_b \qquad \text{and} \qquad A_X + A_a = A_Y + A_b. \tag{6.2}$$

If a or b are non-nuclear particles then $A_i = 0$, while for reactions involving weak interactions the lepton number must also be conserved during the reaction. Therefore any three of the reactants uniquely determine the fourth.

6.1.1 Nuclear energy production

The masses of atomic nuclei are not exactly equal to the sum of the masses of the individual nucleons (protons and neutrons), because the nucleons are bound together by the strong nuclear force. If m_i denotes the mass of a nucleus i, then the *binding energy* of the nucleus can be defined as

$$E_{B,i} = [(A_i - Z_i)m_\mathrm{n} + Z_i m_\mathrm{p} - m_i]\, c^2, \tag{6.3}$$

where m_n and m_p are the masses of a free neutron and proton respectively. Therefore, although $\sum A_i$ is conserved during a nuclear reaction, the sum of the actual masses involved in the reaction is not. This mass difference Δm is converted into energy according to Einstein's formula $E = \Delta m c^2$. The energy released by a reaction of the kind $X(a,b)Y$ is therefore

$$Q = (m_X + m_a - m_Y - m_b)\, c^2. \tag{6.4}$$

Note that Q may be negative if energy is absorbed by the reaction; such reactions are called *endothermic*. Reactions that release energy ($Q > 0$) are called *exothermic*.

In practice, one often uses atomic masses rather than nuclear masses to calculate Q. This is allowed because the number of electrons is conserved during a reaction – despite the fact that the nuclei are completely ionized under the conditions where nuclear reactions take place. Atomic masses of a few important isotopes are given in Table 6.1. The energy release by a reaction is related to the so-called *mass defect* of nuclei, defined as

$$\Delta M_i = (m_i - A_i m_\mathrm{u})\, c^2. \tag{6.5}$$

Since nucleon number is conserved during a reaction, we can write (6.4) as

$$Q = \Delta M_X + \Delta M_a - \Delta M_Y - \Delta M_b. \tag{6.6}$$

Nuclear binding energies and reaction Q-values are usually expressed in MeV. Published tables of atomic masses often list the mass defects in MeV, rather than the masses themselves. Remember that m_u is defined as 1/12 times the mass of the ^{12}C atom; a useful identity is $m_\mathrm{u}c^2 = 931.494\,\mathrm{MeV}$.

When comparing different nuclei, the *binding energy per nucleon* E_B/A is a more informative quantity than E_B itself. In Fig. 6.1 this quantity is plotted against mass number A. With the exception of the lightest nuclei, typical values are around 8 MeV. This reflects the short range of the strong nuclear force: a nucleon only 'feels' the attraction of the nucleons in its immediate vicinity, so that E_B/A quickly saturates with increasing A. There is a slow increase with A up to a maximum at ^{56}Fe,

Table 6.1. Atomic masses of several important isotopes.

element	Z	A	M/m_u	element	Z	A	M/m_u	element	Z	A	M/m_u
n	0	1	1.008665	C	6	12	12.000000	Ne	10	20	19.992441
H	1	1	1.007825		6	13	13.003354	Mg	12	24	23.985043
	1	2	2.014101	N	7	13	13.005738	Si	14	28	27.976930
He	2	3	3.016029		7	14	14.003074	Fe	26	56	55.934940
	2	4	4.002603		7	15	15.000108	Ni	28	56	55.942139
Li	3	6	6.015124	O	8	15	15.003070				
	3	7	7.016003		8	16	15.994915				
Be	4	7	7.016928		8	17	16.999133				
	4	8	8.005308		8	18	17.999160				

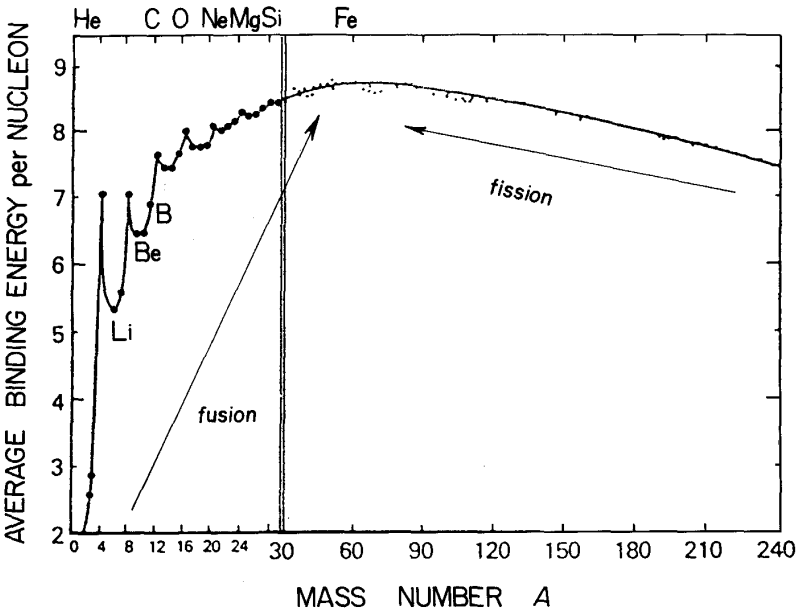

Figure 6.1. Binding energy of atomic nuclei per nucleon, E_B/A as a function of mass number A.

which has $E_B/A = 8.79\,\mathrm{MeV}$, beyond which the binding energy per nucleon decreases towards larger A. This decrease is due to the increase in the number of protons Z with A: the protons inside the nucleus experience a repulsive Coulomb force, which has a long range and does not saturate with increasing Z. There is additional structure in the curve, caused by the shell structure of nuclei and pairing effects.

The most tightly bound nuclei occur around the maximum at ^{56}Fe. Energy can be gained from the fusion of light nuclei into heavier ones as long as E_B/A increases; this is the main energy source in stars. Fusion of nuclei heavier than ^{56}Fe would be endothermic and does not occur in nature (but energy can be released by fission reactions that break up heavy nuclei into lighter ones). ^{56}Fe thus forms the natural endpoint of the stellar nuclear reaction cycles. In a star initially consisting mostly of hydrogen, each step in the transformation of H into Fe releases energy: a total of 8.8 MeV per nucleon, of which 7.0 MeV are already used up in the first step, the fusion of H into He.

6.2 Thermonuclear reaction rates

Consider again a reaction of the type $X(a,b)Y$. Let us first suppose that particles X are bombarded by particles a with a particular velocity υ. The rate at which they react then depends on the *cross-section*, i.e. the effective surface area of the particle X for interacting with particle a. The cross-section is defined as

$$\sigma = \frac{\text{number of reactions } X(a,b)Y \text{ per second}}{\text{flux of incident particles } a},$$

which indeed has a unit of area (cm^2). We denote the reacting particles X and a by indices i and j and their number densities as n_i and n_j, respectively. The incident flux of particles a is then $n_j\,\upsilon$, so that the number of reactions with a certain particle X taking place per second is $n_j\,\upsilon\,\sigma$. The number of reactions per second in a unit volume is therefore

$$\tilde{r}_{ij} = n_i n_j\,\upsilon\,\sigma,$$

which defines the reaction rate at a particular relative velocity υ. This expression applies if X and a are of a different kind. If the reacting particles are identical, then the number of possible reacting

pairs is not $n_i n_j$ but $\frac{1}{2}n_i(n_i-1) \approx \frac{1}{2}n_i^2$ for large particle numbers. Thus we can write more generally

$$\tilde{r}_{ij} = \frac{1}{1+\delta_{ij}} n_i n_j \, \upsilon \, \sigma, \tag{6.7}$$

since $\delta_{ij} = 0$ if $i \neq j$ and $\delta_{ij} = 1$ if $i = j$.

In general, $\sigma = \sigma(\upsilon)$ depends on the relative velocity. In a stellar gas there is a distribution of velocities $\phi(\upsilon)$, normalized such that $\int_o^\infty \phi(\upsilon)\,\mathrm{d}\upsilon = 1$. The overall reaction rate, i.e the number of reactions taking place per second and per unit volume, is therefore

$$r_{ij} = \frac{1}{1+\delta_{ij}} \, n_i n_j \int_0^\infty \phi(\upsilon)\,\sigma(\upsilon)\upsilon \,\mathrm{d}\upsilon = \frac{1}{1+\delta_{ij}} \, n_i n_j \langle \sigma\upsilon \rangle. \tag{6.8}$$

In an ideal gas in LTE, the particle velocities are given by the Maxwell-Boltzmann distribution, eq. (3.13). If each particle velocity distribution is Maxwellian, then so is their *relative* velocity distribution,

$$\phi(\upsilon) = 4\pi\upsilon^2 \left(\frac{m}{2\pi kT}\right)^{3/2} \exp\left(-\frac{m\upsilon^2}{2kT}\right), \tag{6.9}$$

where m is the reduced mass in the centre-of-mass frame of the particles,

$$m = \frac{m_i m_j}{m_i + m_j}. \tag{6.10}$$

We replace the relative velocity υ by the kinetic energy in the centre-of-mass frame, $E = \frac{1}{2}m\upsilon^2$. Using the fact that $\phi(\upsilon)\,\mathrm{d}\upsilon = \phi(E)\,\mathrm{d}E$, we can write the average over $\sigma\upsilon$ in eq. (6.8) as

$$\langle \sigma\upsilon \rangle = \left(\frac{8}{\pi m}\right)^{1/2} (kT)^{-3/2} \int_0^\infty \sigma(E)\, E \, \exp\left(-\frac{E}{kT}\right) \mathrm{d}E. \tag{6.11}$$

This depends only on temperature, i.e. the dependence on velocity in eq. (6.7) turns into a dependence on the *temperature* in the overall reaction rate. The temperature dependence of a nuclear reaction is thus expressed by the factor $\langle \sigma\upsilon \rangle$. To understand this temperature dependence, we must consider in more detail the reaction cross sections and their dependence on energy.

6.2.1 Nuclear cross-sections

The cross-section σ appearing in the reaction rate equation (6.8) is a measure of the probability that a nuclear reaction occurs, given the number densities of the reacting nuclei. While the energy gain from a reaction can be simply calculated from the mass deficits of the nuclei, the cross-section is much more difficult to obtain. Classically, the geometrical cross-section for a reaction between nuclei i and j with radii R_i and R_j is $\sigma = \pi(R_i + R_j)^2$. A good approximation to the nuclear 'radius', or rather for the range of the nuclear force, is

$$R_i \approx R_0 A_i^{1/3} \qquad \text{with} \qquad R_0 = 1.44 \times 10^{-13}\,\mathrm{cm}. \tag{6.12}$$

This would yield typical cross-sections of the order of 10^{-25}–$10^{-24}\,\mathrm{cm}^2$. On the other hand, quantum-mechanically the particles 'see' each other as smeared out over a length equal to the de Broglie wavelength associated with their relative momentum p,

$$\lambda = \frac{\hbar}{p} = \frac{\hbar}{(2mE)^{1/2}}, \tag{6.13}$$

with m and E the reduced mass and relative kinetic energy as defined before. The last equality assumes non-relativistic particles. A better estimate of the geometrical cross-section is therefore $\sigma = \pi\lambda^2$. At typical conditions in the stellar gas, this is (much) larger than the classical estimate since $\lambda > R_i + R_j$. The real situation is much more complicated owing to a number of effects:

- Charged nuclei experience a repulsive Coulomb force which, although weaker than the strong nuclear force, has a much longer range. This Coulomb barrier would prevent any reaction to occur under stellar condition, were it not for the quantum-mechanical *tunnel effect*.
- The nature of the force involved in the reaction determines the strength of the interaction. For a reaction $X(a,b)Y$, the emitted particle may be either another nucleus, a γ-photon, or an $e^-\overline{\nu}$ or $e^+\nu$ pair. In the first case, only the strong force is involved and the cross-section may be close to the geometrical one. The second case also involves the electromagnetic force, which is weaker and gives a lower reaction probability, i.e. a smaller cross-section. In the last case, a weak interaction must occur which has an even lower probability and smaller cross-section.
- Nuclear structure effects can have a strong influence on the cross-section. This is particularly true in the case of *resonant interactions*.

Coulomb barrier and the tunnel effect

At distances r larger than the range of the nuclear force, two nuclei with charges Z_i and Z_j experience a repulsive Coulomb potential

$$V(r) = \frac{Z_i Z_j e^2}{r} = 1.44 \frac{Z_i Z_j}{r\,[\mathrm{fm}]}\,\mathrm{MeV}, \tag{6.14}$$

with r expressed in fm = 10^{-13} cm in the last equality. To experience the attractive nuclear force the particles have to approach each other within a typical distance $r_\mathrm{n} \sim A^{1/3} R_0$ as given by eq. (6.12). For $r < r_\mathrm{n}$ the nuclear attraction gives a potential drop to roughly $V_0 \approx -30$ MeV. The particles must therefore overcome a typical Coulomb barrier $E_\mathrm{C} = V(r_\mathrm{n}) \approx Z_1 Z_2$ MeV, see Fig. 6.2.

If an incoming particle has a kinetic energy E at infinity in the reference frame of the nucleus, it can classically only come within a distance r_c given by $E = V(r_\mathrm{c})$. In stellar interiors the kinetic energies of nuclei have a Maxwellian distribution, with an average value $\langle E \rangle = \frac{3}{2}kT \approx 1.3$ keV at 10^7 K, which is typical of the centre of the Sun and other main-sequence stars. This falls short of the Coulomb barrier by a factor of about 1000. Even considering the high-energy tail of the Maxwell-Boltzmann distribution, the fraction of particles with $E > E_\mathrm{C}$ is vanishingly small. With purely classical considerations nuclear reactions have no chance of happening at such temperatures.

We need to turn to quantum mechanics to see how nuclear reactions are possible at stellar temperatures. As was discovered by G. Gamow, there is a finite probability that the projectile penetrates the repulsive Coulomb barrier even if $E \ll E_\mathrm{C}$. The tunnelling probability can be estimated as

$$P \sim \exp\left(- \int_{r_\mathrm{n}}^{r_\mathrm{c}} \frac{\sqrt{2m[V(r) - E]}}{\hbar}\,\mathrm{d}r \right)$$

where

$$r_\mathrm{c} = \frac{Z_i Z_j e^2}{E}$$

is the classical distance of closest approach. The result is

$$P = P_0 \exp(-b\,E^{-1/2}) \qquad \text{with} \qquad b = 2\pi \frac{Z_i Z_j e^2}{\hbar} \left(\frac{m}{2}\right)^{1/2} = 31.29\, Z_i Z_j A^{1/2}\,[\mathrm{keV}]^{1/2}. \tag{6.15}$$

Here $A = A_i A_j/(A_i + A_j)$ is the reduced mass in units of m_u and P_0 is a constant. P increases steeply with E and decreases with $Z_i Z_j$, i.e., with the height of the Coulomb barrier. Therefore, at relative low temperatures only the lightest nuclei (with the smallest $Z_i Z_j$) have a non-negligible chance to react. Reactions with heavier nuclei, with larger $Z_i Z_j$, require larger energies and therefore higher temperatures to have a comparable penetration probability.

Nuclear structure effects on the cross-section

A typical thermonuclear reaction proceeds as follows. After penetrating the Coulomb barrier, the two nuclei can from an unstable, excited *compound nucleus* which after a short time decays into the product particles, e.g.

$$X + a \rightarrow C^* \rightarrow Y + b\,.$$

Although the lifetime of the compound nucleus C^* is very short, it is much longer than the crossing time of the nucleus at the speed of light ($\sim 10^{-21}$ s). Therefore by the time it decays, the compound nucleus has no 'memory' of how it was formed, and the decay depends only on the energy.

The decay can proceed via different channels, e.g. $C^* \rightarrow X + a$, $\rightarrow Y_1 + b_1$, $\rightarrow Y_2 + b_2$, $\ldots$, $\rightarrow C + \gamma$. In the first case the original particles are reproduced, the last case is a decay to a stable energy level of C with γ-emission. In the other cases the particles b_1, b_2, etc. may be protons, neutrons or α-particles. (Reactions involving electron and neutrino emission do not proceed via a compound intermediate state, since the necessary β-decays would be prohibitively slow.) In order for a certain energy level of C^* to decay via a certain channel, the conservations laws of energy, momentum, angular momentum and nuclear symmetries must be fulfilled. The outgoing particles obtain a certain kinetic energy, which – with the exception of neutrinos that escape without interaction – is quickly thermalised, i.e. shared among the other gas particles owing to the short photon and particle mean free paths in the stellar gas.

The energy levels of the compound nucleus play a crucial role in determining the reaction cross-section, see Fig. 6.2. Let $E_{\rm min}$ be the minimum energy required to remove a nucleon from the ground state of C to infinity, analogous to the ionization energy of an atom. Energy levels below $E_{\rm min}$ correspond to bound states in an atom; these can only decay by γ-emission which is relatively improbable. These 'stationary' energy levels have long lifetimes τ and correspondingly small widths Γ, since according to Heisenberg's uncertainty relation

$$\Gamma = \frac{\hbar}{\tau}. \tag{6.16}$$

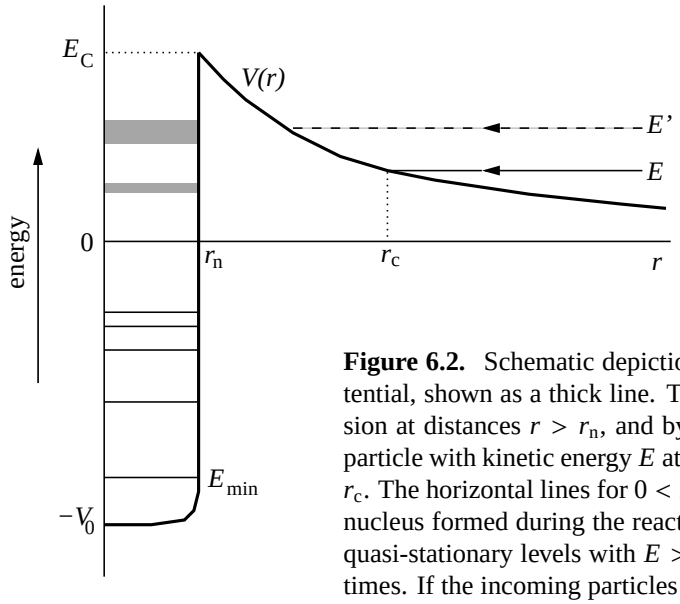

Figure 6.2. Schematic depiction of the combined nuclear and Coulomb potential, shown as a thick line. The potential is dominated by Coulomb repulsion at distances $r > r_{\rm n}$, and by nuclear attraction for $r < r_{\rm n}$. An incoming particle with kinetic energy E at infinity can classically approach to a distance $r_{\rm c}$. The horizontal lines for $0 < r < r_{\rm n}$ indicate energy levels in the compound nucleus formed during the reaction. The ground state is at energy $-E_{\rm min}$; the quasi-stationary levels with $E > 0$ are broadened due to their very short lifetimes. If the incoming particles have energy E' corresponding to such a level they can find a resonance in the compound nucleus (see text).

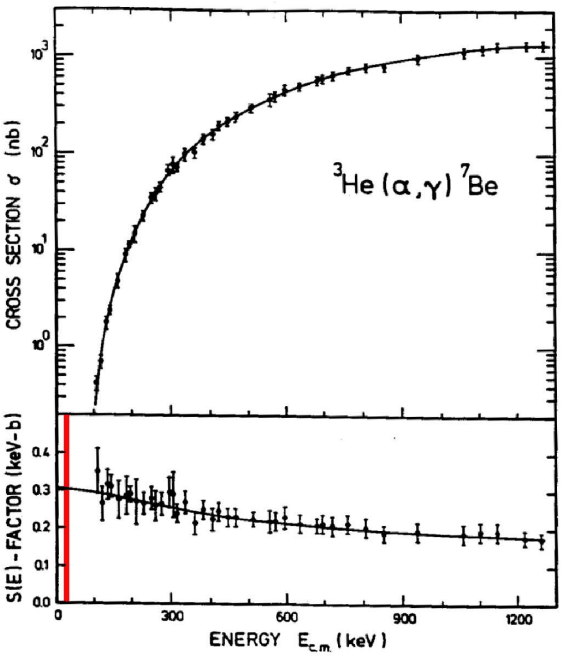

Figure 6.3. Example of the dependence of the reaction cross section on energy E for the ^{3}He + ^{4}He $\rightarrow$ ^{7}Be + γ reaction. Although σ varies very strongly with energy, and becomes immeasurably small at very low E, the factor $S(E)$ is only a very weak function of E and – at least for this reaction – can be safely extrapolated to the low energies that are relevant for nuclear reactions in stars (15–30 keV, vertical bar on the left).

Energy levels above $E_{\rm min}$ can also expel particles, which is much more probable than γ-emission. These levels also have finite lifetimes because of the sharp potential rise beyond $r_{\rm n}$, but eventually the particles can escape by the tunnel effect. These 'quasi-stationary' levels have much shorter lifetimes and correspondingly larger widths. The probability of escape increases with energy and so does the level width, until eventually Γ is larger than the distance between levels resulting in a continuum of energy states above a certain $E_{\rm max}$.

The possible existence of discrete energy levels above $E_{\rm min}$ can give rise to so-called 'resonances' with much increased reaction probabilities. Suppose we let X and a react with gradually increasing relative energy E (measured at large distance). As long as E is in a region without or in between quasi-stationary levels, the reaction probability will simply increase with the penetration probability (6.15). However, if E coincides with such a level (e.g. energy E' in Fig. 6.2), then the reaction probability can be enhanced by several orders of magnitude. For energies close to such a level $E_{\rm res}$ the cross-section has an energy dependence with a typical resonance form,

$$\xi(E) \propto \frac{1}{(E - E_{\rm res})^2 + (\Gamma/2)^2}. \tag{6.17}$$

At $E = E_{\rm res}$ the cross-section can be close to the geometrical cross-section, $\pi\lambda^2$, where λ is the de Broglie wavelength (6.13). We can thus expect the cross-section to depend on energy as

$$\sigma(E) \propto \pi\lambda^2\, P(E)\, \xi(E). \tag{6.18}$$

The astrophysical cross-section factor

Since $\lambda^2 \propto 1/E$ and $P(E) \propto \exp(-b\,E^{-1/2})$, one usually writes

$$\boxed{\sigma(E) = S(E)\,\frac{\exp(-b\,E^{-1/2})}{E}}\,. \tag{6.19}$$

This equation defines the 'astrophysical S-factor' $S(E)$, which contains all remaining effects, i.e. the intrinsic nuclear properties of the reaction including possible resonances.

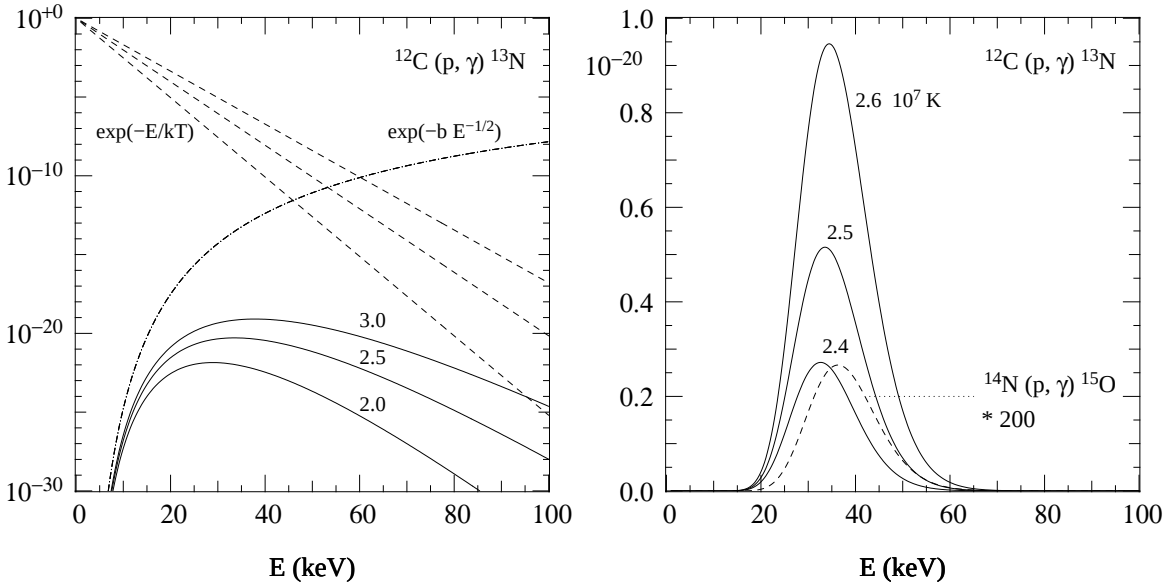

Figure 6.4. Example of the Gamow peak for the ^{12}C(p, γ)^{13}N reaction. The left panel shows as dash-dotted lines the tunnelling probability factor, $\exp(-b/E^{1/2})$, and as dashed lines the tail of the Maxwell distribution, $\exp(-E/kT)$, for three values of temperature: $T = 2.0{\times}10^7$ K (lower curve), $2.5{\times}10^7$ K (middle) and $3.0{\times}10^7$ K (upper). The solid lines show the product of these two factors, $f(E)$ as in eq. (6.21), labelled by $T_7 \equiv T/10^7$ K. Note the enormous range of the vertical log-scale. To appreciate the sharpness of the Gamow peak, and the enormous sensitivity to temperature, the right panel shows $f(E)$ on a linear scale for $T_7 = 2.4$, 2.5 and 2.6. The dashed line is the Gamow peak for the ^{14}N(p, γ)^{15}O reaction for $T_7 = 2.4$, multiplied by a factor 200.

The S-factor can in principle be calculated, but in practice one relies on laboratory measurements of the cross-section to obtain $S(E)$. The difficulty is that such measurements are only feasible at large E, typically > 0.1 MeV, because cross-sections quickly become unmeasurably small at lower energies. This lowest energy is still an order of magnitude larger than the energies at which reactions typically take place under stellar conditions. One therefore has to extrapolate $S(E)$ down over quite a large range of E to the relevant energies. In many cases $S(E)$ is nearly constant or varies slowly with E – unlike $\sigma(E)$! – and this procedure can be quite reliable (e.g. see Fig. 6.3). However, when resonances occur in the range of energies over which to extrapolate, the results can be very uncertain.

6.2.2 Temperature dependence of reaction rates

Combining eqs. (6.11) and (6.19), the cross-section factor $\langle\sigma\upsilon\rangle$ can be written as

$$\langle\sigma\upsilon\rangle \;=\; (8/\pi m)^{1/2}(kT)^{-3/2} \int_0^\infty S(E)\,\exp\!\left(-\frac{E}{kT}-\frac{b}{E^{1/2}}\right)\mathrm{d}E. \tag{6.20}$$

We will look at the case of *non-resonant* reactions, where we can assume that $S(E)$ varies slowly with E. The integrand is then dominated by the product of two exponential factors: $\exp(-E/kT)$, the tail of the Maxwell-Boltzmann distribution which decreases rapidly with E; and $\exp(-bE^{-1/2})$, the penetration probability due to the tunnel effect which increases rapidly with E. The product of these two exponentials,

$$f(E) = \exp\!\left(-\frac{E}{kT}-\frac{b}{E^{1/2}}\right), \tag{6.21}$$

is a sharply peaked function called the *Gamow peak*, which has appreciable values only around a maximum at energy E_0. Fig. 6.4 shows an example for the reaction $^{12}\mathrm{C} + \mathrm{p} \rightarrow {}^{13}\mathrm{N} + \gamma$. Since by assumption $S(E)$ varies slowly with E, we can take $S(E) \approx S(E_0)$ out of the integral (6.20) and obtain

$$\langle \sigma \upsilon \rangle \approx (8/\pi m)^{1/2} (kT)^{-3/2} S(E_0) \int_0^\infty \exp\left(-\frac{E}{kT} - \frac{b}{E^{1/2}} \right) \mathrm{d}E. \tag{6.22}$$

The reaction rate then only depends on the integral $\int_0^\infty f(E)\,\mathrm{d}E$.

Properties of the Gamow peak

The value of the Gamow peak energy E_0 can be found by taking $\mathrm{d}f/\mathrm{d}E = 0$, which gives

$$E_0 = (\tfrac{1}{2} bkT)^{2/3} = 5.665\,(Z_i^2 Z_j^2 A\, T_7^2)^{1/3}\,\mathrm{keV}. \tag{6.23}$$

To obtain the last equality we have substituted b as given by eq. (6.15) and we use the notation $T_n = T/(10^n\,\mathrm{K})$, while A is the reduced mass in m_u as before. For reactions between light nuclei at temperatures $T \sim 1\text{–}2 \times 10^7\,\mathrm{K}$, $E_0 \sim 10\text{–}30\,\mathrm{keV}$, while the average kinetic energies are 1–2 keV. The peak is quite narrow, having a width ΔE at half maximum that is always smaller than E_0. Thus, the nuclei that contribute to the reaction rate have energies in a narrow interval around 10 times the thermal energy, but about 2 orders of magnitude below the Coulomb barrier.

The right panel of Fig. 6.4 illustrates the strong dependence of the maximum value $f(E_0)$ of the Gamow peak on the temperature. In the case of the $^{12}\mathrm{C}(\mathrm{p},\gamma)^{13}\mathrm{N}$ reaction, an increase in temperature by 4% (from $T_7 = 2.4$ to 2.5, or from 2.5 to 2.6) almost doubles the maximum value of $f(E)$. The width of the peak also increases modestly, such that the area under the curve – which is the integral that appears in eq. (6.22) – increases enormously with increasing temperature. This is the reason why thermonuclear reaction rates are extremely sensitive to the temperature.

When we compare different reactions, the factor $b \propto Z_1 Z_2 A^{1/2}$ changes and thereby the penetration probability at a certain energy. A reaction between heavier nuclei (with larger A and Z) will therefore have a much lower rate at certain fixed temperature. This is illustrated in the right panel of Fig. 6.4 by the dashed curve, showing the Gamow peak for the $^{14}\mathrm{N}(\mathrm{p},\gamma)^{15}\mathrm{O}$ reaction at $T_7 = 2.4$, multiplied by a factor 200. Hence, the probability of this reaction is 200 times smaller than that of the $^{12}\mathrm{C}(\mathrm{p},\gamma)^{13}\mathrm{N}$ reaction at the same temperature. In other words, reactions between heavier nuclei will need a higher temperature to occur at an appreciable rate.

To summarize, the properties of the Gamow peak imply that

- the reaction rate $\langle \sigma \upsilon \rangle$ increases *very strongly with temperature*.
- $\langle \sigma \upsilon \rangle$ decreases strongly with increasing Coulomb barrier.

Analytic expressions for the temperature dependence

We can find an analytical expression for the reaction rate if we approximate the integrand $f(E)$ in eq. (6.22) by a Gaussian centred at E_0, i.e.,

$$f(E) \approx f(E_0) \exp\left[-\left(\frac{E - E_0}{\Delta E} \right)^2 \right], \tag{6.24}$$

Considering the shapes of the curves in Fig. 6.4, this is not a bad approximation. From eq. (6.21) we find $f(E_0) = \exp(-3E_0/kT) \equiv \exp(-\tau)$, which defines the often used quantity τ,

$$\tau = \frac{3E_0}{kT} = 19.72 \left(\frac{Z_i^2 Z_j^2 A}{T_7} \right)^{1/3}. \tag{6.25}$$

The width ΔE of the Gaussian can be obtained by expanding eq. (6.21) for $f(E)$ in a Taylor series around E_0,

$$f(E) = f(E_0) + f'(E_0)\,(E - E_0) + \tfrac{1}{2} f''(E_0)\,(E - E_0)^2 + \ldots,$$

in which the second term equals zero because $f'(E_0) = 0$. Comparing this with a similar expansion of the Gaussian approximation to $f(E)$ yields the same expression, to second order, if

$$\Delta E = \left(\frac{-2f}{f''}\right)^{1/2}_{E=E_0} = \left(\frac{4E_0 kT}{3}\right)^{1/2} \tag{6.26}$$

We can then approximate the integral in eq. (6.22) by

$$\int_0^\infty f(E)\,\mathrm{d}E \;\approx\; e^{-\tau} \int_0^\infty \exp\left[-\left(\frac{E - E_0}{\Delta E}\right)^2\right] \mathrm{d}E \;\approx\; e^{-\tau}\,\sqrt{\pi}\,\Delta E. \tag{6.27}$$

In the last step we have extended the integral from $-\infty$ to ∞ to obtain the result $\sqrt{\pi}\,\Delta E$, which introduces only a very small error because the exponential is negligibly small for $E < 0$. When we substitute (6.27) with the expression (6.26) for ΔE into (6.22), and we eliminate E_0 and kT in favour of τ and b using (6.23) and (6.25), then we find after some manipulation

$$\langle \sigma v \rangle \;\approx\; \frac{8}{9}\left(\frac{2}{3m}\right)^{1/2} \frac{S(E_0)}{b}\,\tau^2\,e^{-\tau} \;=\; \frac{7.21 \times 10^5}{Z_i Z_j A}\left(\frac{S(E_0)}{\mathrm{keV\,cm^2}}\right)\tau^2\,e^{-\tau}. \tag{6.28}$$

In the last equality we have substituted the explicit expression (6.15) for b. Since $\tau \propto T^{-1/3}$ this gives a temperature dependence of the form

$$\langle \sigma v \rangle \propto \frac{1}{T^{2/3}}\,\exp\left(-\frac{C}{T^{1/3}}\right), \tag{6.29}$$

where the constant C in the exponential factor depends on $Z_i Z_j$, i.e. on the height of the Coulomb barrier. This is indeed a strongly increasing function of temperature.

If we consider a small range of temperatures around some value T_0, we can write

$$\langle \sigma v \rangle = \langle \sigma v \rangle_0 \left(\frac{T}{T_0}\right)^\nu \qquad \text{with} \qquad \nu \equiv \frac{\partial \log\langle \sigma v \rangle}{\partial \log T} = \frac{\tau - 2}{3}. \tag{6.30}$$

The last equality follows from (6.28) and (6.25). Therefore the exponent ν is not a constant but depends on T itself – in fact ν decreases with T roughly as $T^{-1/3}$. In general, however, any particular reaction is only important in quite a limited range of temperatures, so that taking ν as constant in (6.30) is approximately correct. Values of the exponent ν are in all cases $\gg 1$. For example, at $T_7 = 1.5$ we find $\langle \sigma v \rangle \propto T^{3.9}$ for the p + p reaction for hydrogen fusion and $\langle \sigma v \rangle \propto T^{20}$ for the $^{14}\mathrm{N(p,\gamma)}$ reaction in the CNO cycle (see Sec. 6.4.1). Thus thermonuclear reaction rates are about the most strongly varying functions found in physics. This temperature sensitivity has a strong influence on stellar models, as we shall see.

6.2.3 Electron screening

We found that the repulsive Coulomb force between nuclei plays a crucial role in determining the rate of a thermonuclear reaction. In our derivation of the cross section we have ignored the influence of the surrounding free electrons, which provide overall charge neutrality in the gas. In a dense medium, the attractive Coulomb interactions between atomic nuclei and free electrons cause each nucleus to

be effectively surrounded by a cloud of electrons. This electron cloud reduces the Coulomb repulsion between the nuclei at large distances, and may thus increase the probability of tunneling through the Coulomb barrier. This effect is know as *electron screening* or *electron shielding*.

We simply give the main results, the derivation of which can be found in MAEDER Sec. 9.4 or KIPPENHAHN Sec. 18.4. The repulsive Coulomb potential (eq. 6.14) is reduced by a factor $\exp(-r/r_{\rm D})$, where $r_{\rm D}$, the so-called Debye-Hückel radius, represents the effective radius of the electron cloud. The stronger the Coulomb interactions between nuclei and electrons, the smaller $r_{\rm D}$. We have found (Sec. 3.6.1) that Coulomb interactions increase in strength with increasing density and decreasing temperature, and so does the magnitude of the electron screening effect. It turns out that the reaction rate $\langle\sigma\upsilon\rangle$ is enhanced by a factor

$$f = \exp\left(\frac{E_{\rm D}}{kT}\right), \tag{6.31}$$

where, for small values of $E_{\rm D}/kT \ll 1$,

$$\frac{E_{\rm D}}{kT} = \frac{Z_1 Z_2 e^2}{r_{\rm D} kT} \sim 0.006\, Z_1 Z_2\, \frac{\rho^{1/2}}{{T_7}^{3/2}}. \tag{6.32}$$

This is the *weak screening* approximation, which applies to relatively low densities and high temperatures such as found in the centre of the Sun and other main-sequence stars. Under these conditions, reaction rates are enhanced only by modest factors, $f \lesssim 1.1$.

The description of electron screening becomes complicated at high densities and relatively low temperatures, where the weak screening approximation is no longer valid. A general result is that with increasing strength of electron screening, the temperature sensitivity of the reaction rate diminishes and the density dependence becomes stronger. At very high densities, $\rho \gtrsim 10^6$ g/cm^3, the screening effect is so large that it becomes the dominating factor in the reaction rate. The shielding of the Coulomb barrier can be so effective that the reaction rate depends mainly on the density and no longer on temperature. Reactions between charged nuclei become possible even at low temperature, if the density exceeds a certain threshold. One then speaks of *pycnonuclear reactions*, which can play an important role in late stages of stellar evolution. In a very cool and dense medium one must also take into account the effect of crystallization, which decreases the mobility of the nuclei and thus the probability of collisions.

6.3 Energy generation rates and composition changes

Having obtained an expression for the cross-section factor $\langle\sigma\upsilon\rangle$, the reaction rate r_{ij} follows from eq. (6.8). We can then easily obtain the energy generation rate. Each reaction releases an amount of energy Q_{ij} according to eq. (6.4), so that $Q_{ij}\, r_{ij}$ is the energy generated per unit volume and per second. The energy generation rate per *unit mass* from the reaction between nuclei of type i and j is then

$$\epsilon_{ij} = \frac{Q_{ij}\, r_{ij}}{\rho}. \tag{6.33}$$

We can express the energy generation rate in terms of the mass fractions X_i and X_j and the density ρ using eq. (6.8). Replacing the number density n_i by the mass fraction X_i according to $n_i = X_i\,\rho/(A_i m_u)$, eq. (6.33) can be written as

$$\epsilon_{ij} = \frac{Q_{ij}}{(1+\delta_{ij})\, A_i A_j m_{\rm u}^2}\, \rho\, X_i X_j\, \langle\sigma\upsilon\rangle_{ij} = \frac{q_{ij}}{(1+\delta_{ij})\, A m_{\rm u}}\, \rho\, X_i X_j\, \langle\sigma\upsilon\rangle_{ij}, \tag{6.34}$$

In the last identity $A = A_i A_j/(A_i + A_j)$ is the reduced mass in units of m_u, and we have replaced Q_{ij} by the energy released per unit mass by this reaction

$$q_{ij} = \frac{Q_{ij}}{m_i + m_j} \approx \frac{Q_{ij}}{(A_i + A_j)m_\mathrm{u}}. \tag{6.35}$$

Remember that $\langle\sigma\upsilon\rangle$ contains the temperature dependence of the reaction rate. If we use the power-law approximation (6.30) we can write the energy generation rate of a reaction as

$$\epsilon_{ij} = \epsilon_{0,ij}\, X_i X_j\, \rho\, T^\nu. \tag{6.36}$$

The total nuclear energy generation rate results from all reactions taking place in a certain mass element in the star, i.e.

$$\epsilon_\mathrm{nuc} = \sum_{i,j} \epsilon_{ij}. \tag{6.37}$$

This is the quantity ϵ_nuc that appears in the stellar structure equation for the luminosity, eq. (5.4).

Composition changes

The reaction rates also determine the rate at which the composition changes. The rate of change in the number density n_i of nuclei of type i owing to reactions with nuclei of type j is

$$\left(\frac{\mathrm{d}n_i}{\mathrm{d}t}\right)_j = -(1+\delta_{ij})\, r_{ij} = -n_i n_j\, \langle\sigma\upsilon\rangle_{ij}. \tag{6.38}$$

The factor $1+\delta_{ij}$ takes into account that a reaction between identical nuclei consumes *two* such nuclei. One can define the *nuclear lifetime* of a species i owing to reactions with j as

$$\tau_{i,j} = \frac{n_i}{|(\mathrm{d}n_i/\mathrm{d}t)_j|} = \frac{1}{n_j\, \langle\sigma\upsilon\rangle_{ij}}, \tag{6.39}$$

which is the timescale on which the abundance of i changes as a result of this reaction.

The overall change in the number n_i of nuclei of type i in a unit volume can generally be the result of different nuclear reactions. Some reactions (with rate r_{ij} as defined above) consume i while other reactions, e.g. between nuclei k and l, may produce i. If we denote the rate of reactions of the latter type as $r_{kl,i}$, we can write for the total rate of change of n_i:

$$\frac{\mathrm{d}n_i}{\mathrm{d}t} = -\sum_j (1+\delta_{ij})\, r_{ij} + \sum_{k,l} r_{kl,i} \tag{6.40}$$

The number density n_i is related to the mass fraction X_i by $n_i = X_i\,\rho/(A_i m_u)$, so that we can write the rate of change of the mass fraction due to nuclear reactions as

$$\frac{\mathrm{d}X_i}{\mathrm{d}t} = A_i \frac{m_\mathrm{u}}{\rho}\left(-\sum_j (1+\delta_{ij})\, r_{ij} + \sum_{k,l} r_{kl,i}\right) \tag{6.41}$$

For each nuclear species i one can write such an equation, describing the composition change at a particular mass shell inside the star (with density ρ and temperature T) resulting from nuclear reactions. In the presence of internal mixing (in particular of *convection*, Sec. 5.5.3) the redistribution of composition between different mass shells should also be taken into account.

Note the similarity between the expressions for the nuclear energy generation rate (6.37) and the equation for composition changes (6.41), both of which are proportional to r_{ij}. Using eq. (6.35) for the energy released per gram, we can write the reaction rate as

$$r_{ij} = \frac{\epsilon_{ij}}{q_{ij}(A_i + A_j)} \frac{\rho}{m_\mathrm{u}}. \tag{6.42}$$

If we substitute this expression into eq. (6.41) the factor ρ/m_u drops out. We obtain a useful expression in simple cases where only *one* reaction occurs, or a reaction chain in which one reaction determines the overall rate. An example is the fusion of $4\,^1\mathrm{H}$ into $^4\mathrm{He}$, which is the net result of a chain of reactions (see Sec. 6.4.1). In that case you may verify that (6.41) and (6.42) reduce to

$$\frac{\mathrm{d}Y}{\mathrm{d}t} = -\frac{\mathrm{d}X}{\mathrm{d}t} = \frac{\epsilon_\mathrm{H}}{q_\mathrm{H}}, \tag{6.43}$$

where ϵ_H is the energy generation rate by the complete chain of H-burning reactions, and q_H is amount of energy produced by converting 1 gram of $^1\mathrm{H}$ into $^4\mathrm{He}$.

6.4 The main nuclear burning cycles

In principle, many different nuclear reactions can occur simultaneously in a stellar interior. If one is interested in following the detailed isotopic abundances produced by all these reactions, or if structural changes occur on a very short timescale, a large network of reactions has to be calculated (as implied by eq. 6.41). However, for the calculation of the structure and evolution of a star usually a much simpler procedure is sufficient, for the following reasons:

- The very strong dependence of nuclear reaction rates on the temperature, combined with the sensitivity to the Coulomb barrier $Z_1 Z_2$, implies that nuclear fusions of different possible fuels – hydrogen, helium, carbon, etc. – are well separated by substantial temperature differences. The evolution of a star therefore proceeds through several distinct *nuclear burning cycles*.
- For each nuclear burning cycle, only a handful of reactions contribute significantly to energy production and/or cause major changes to the overall composition.
- In a chain of subsequent reactions, often one reaction is by far the slowest and determines the rate of the whole chain. Then only the rate of this bottleneck reaction needs to be taken into account.

6.4.1 Hydrogen burning

The net result of hydrogen burning is the fusion of four $^1\mathrm{H}$ nuclei into a $^4\mathrm{He}$ nucleus,

$$4\,^1\mathrm{H} \rightarrow {}^4\mathrm{He} + 2\,\mathrm{e}^+ + 2\,\nu\,. \tag{6.44}$$

You may verify using Sec. 6.1.1 that the total energy release is 26.734 MeV. In order to create a $^4\mathrm{He}$ nucleus two protons have to be converted into neutrons. Therefore two neutrinos are released by weak interactions ($\mathrm{p} \rightarrow \mathrm{n} + \mathrm{e}^+ + \nu$), which escape without interacting with the stellar matter. It is customary not to include the neutrino energies into the overall energy release Q, but to take into account only the energy that is used to heat the stellar gas. This includes energy released in the form of γ-rays (including the γ-rays resulting from pair annihilation after e^+ emission) and in the form of kinetic energies of the resulting nuclei. The effective Q-value of hydrogen burning is therefore somewhat smaller than 26.734 MeV and depends on the reaction in which the neutrinos are emitted.

Since a simultaneous reaction between four protons is extremely unlikely, a chain of reactions is always necessary for hydrogen burning. This can take place in two distinct ways: either direct fusion of protons via the *p-p chain*, or by using already present CNO-nuclei as catalysts in the *CNO cycle*. Hydrogen burning in stars takes place at temperatures ranging between 8×10^6 K and 5.0×10^7 K, depending on stellar mass and evolution stage.

The p-p chains

The first reaction is the so-called p-p reaction:

$$^1\mathrm{H} + {}^1\mathrm{H} \rightarrow {}^2\mathrm{H} + \mathrm{e}^+ + \nu \qquad \text{or} \qquad \mathrm{p} + \mathrm{p} \rightarrow \mathrm{D} + \mathrm{e}^+ + \nu\,. \tag{6.45}$$

This involves the simultaneous β-decay of one of the protons during the strong nuclear interaction. This is very unlikely and the p-p reaction therefore has an extremely small cross-section, about 10^{-20} times that of a typical reaction involving only strong interactions. The reaction rate cannot be measured in the laboratory and is only known from theory.

After some deuterium is produced, it rapidly reacts with another proton to from ^{3}He. Subsequently three different branches are possible to complete the chain towards ^{4}He:

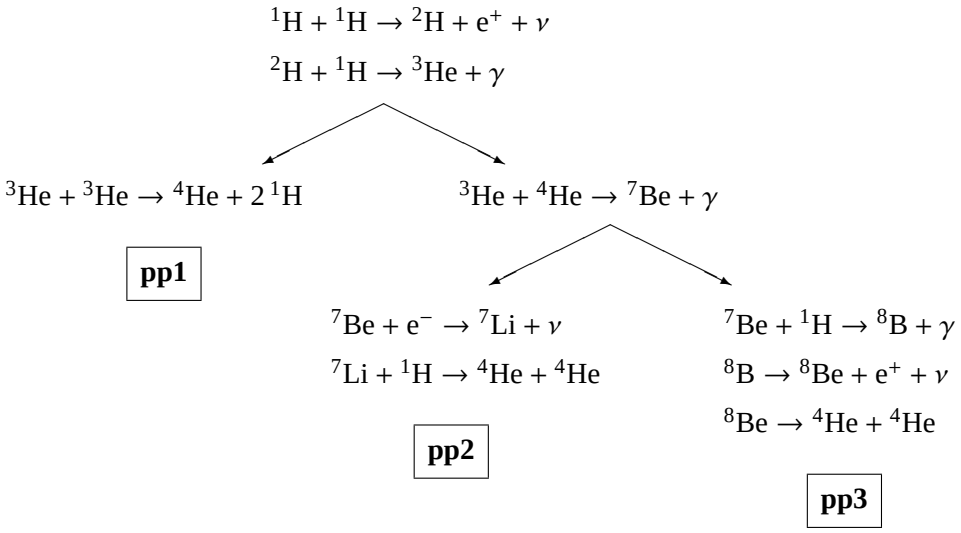

(6.46)

The pp1 branch requires two ^{3}He nuclei, so the first two reactions in the chain have to take place twice. The alternative pp2 and pp3 branches require only one ^{3}He nucleus and an already existing ^{4}He nucleus (either present primordially, or produced previously by hydrogen burning). The resulting ^{7}Be nucleus can either capture an electron or fuse with another proton, giving rise to the second branching into pp2 and pp3. Three of the reactions in the chains are accompanied by neutrino emission, and the (average) neutrino energy is different in each case: $\langle E_\nu \rangle = 0.265$ MeV for the p-p reaction, 0.814 MeV for electron capture of ^{7}Be and 6.71 MeV for the β-decay of ^{8}B. Therefore the total energy release Q_H for the production of one ^{4}He nucleus is different for each chain: 26.20 MeV (pp1), 25.66 MeV (pp2) and only 19.76 MeV for pp3.

The relative frequency of the three chains depends on temperature and chemical composition. Because the ^{3}He + ^{4}He reaction is slightly more sensitive to temperature than the ^{3}He + ^{3}He reaction (it has a somewhat higher reduced mass and larger τ, eq. 6.25), the pp1 chain dominates over the other two at relatively low temperature ($T_7 \lesssim 1.5$). The pp1 chain is the main energy-producing reaction chain in the Sun. At increasing T, first the pp2 chain and then the pp3 chain become increasingly important.

At low temperatures ($T < 8 \times 10^6$ K) the rates of all reactions should be calculated separately to obtain the energy generation rate and the changes in abundances. In particular, the $^3\mathrm{He} + {}^3\mathrm{He}$ reaction is quite slow and a substantial abundance of ^{3}He can accumulate before further reactions occur. For $T \gtrsim 8 \times 10^6$ K all reactions in the chain are fast enough that they reach a steady state, where once a D nucleus is produced by the first, very slow reaction, all successive reactions proceed very quickly until ^{4}He is formed. The nuclear lifetimes (eq. 6.39) of the intermediate nuclei D, ^{3}He, ^{7}Li, etc, are very short compared to the overall nuclear timescale, and their abundances are very small. The overall rate of the whole reaction chain is then set by the rate of the bottleneck p-p reaction, r_{pp}. In this steady-state or 'equilibrium' situation the rate of each subsequent reaction adapts itself to the pp rate.[1] The energy generation rate (given by the sum of energies released by each reaction, eq. 6.37) can then be expressed in a single term of the form (6.33), i.e. $\epsilon_{\mathrm{nuc}} = Q_{\mathrm{H}} r_{\mathrm{pp}}/\rho$ where Q_{H} is the total energy released in the whole chain (6.44). The above expression applies to the pp2 and pp3 chains, which each require one p-p reaction to complete. For the pp1 chain two p-p reactions are needed and therefore in that case $\epsilon_{\mathrm{nuc}} = \frac{1}{2} Q_{\mathrm{H}} r_{\mathrm{pp}}/\rho$. Expressing r_{pp} in terms of the cross section factor $\langle \sigma \upsilon \rangle_{\mathrm{pp}}$ and the hydrogen abundance X, we can compute the energy generation rate for hydrogen burning by the combination of pp chains as

$$\epsilon_{\mathrm{pp}} = \psi \, q_{\mathrm{H}} X^2 \frac{\rho}{m_{\mathrm{u}}} \langle \sigma \upsilon \rangle_{\mathrm{pp}}, \tag{6.47}$$

where $q_{\mathrm{H}} = Q_{\mathrm{H}}/4m_{\mathrm{u}}$ is the total energy release per gram of hydrogen burning and ψ is a factor between 1 (for the pp1 chain) and 2 (for the pp2 and pp3 chains), depending on the relative frequency of the chains. Both ψ and q_{H} therefore depend on the temperature, because the three chains have different neutrino losses. The overall temperature dependence of ϵ_{pp} is dominated by the T-dependence of $\langle \sigma \upsilon \rangle_{\mathrm{pp}}$ and is shown in Fig. 6.5. The pp chain is the least temperature-sensitive of all nuclear burning cycles with a power-law exponent ν (eq. 6.30) varying between about 6 at $T_6 \approx 5$ and 3.5 at $T_6 \approx 20$.

The CNO cycle

If some C, N, and O is already present in the gas out of which a star forms, and if the temperature is sufficiently high, hydrogen fusion can take place via the so-called *CNO cycle*. This is a cyclical sequence of reactions that typically starts with a proton capture by a ^{12}C nucleus, as follows:

$$\begin{aligned}
{}^{12}\mathrm{C} + {}^{1}\mathrm{H} &\rightarrow {}^{13}\mathrm{N} + \gamma \\
{}^{13}\mathrm{N} &\rightarrow {}^{13}\mathrm{C} + \mathrm{e}^+ + \nu \\
{}^{13}\mathrm{C} + {}^{1}\mathrm{H} &\rightarrow {}^{14}\mathrm{N} + \gamma \\
{}^{14}\mathrm{N} + {}^{1}\mathrm{H} &\rightarrow {}^{15}\mathrm{O} + \gamma \\
{}^{15}\mathrm{O} &\rightarrow {}^{15}\mathrm{N} + \mathrm{e}^+ + \nu \\
{}^{15}\mathrm{N} + {}^{1}\mathrm{H} &\rightarrow {}^{12}\mathrm{C} + {}^{4}\mathrm{He} \\
&\rightarrow {}^{16}\mathrm{O} + \gamma \\
{}^{16}\mathrm{O} + {}^{1}\mathrm{H} &\rightarrow {}^{17}\mathrm{F} + \gamma \\
{}^{17}\mathrm{F} &\rightarrow {}^{17}\mathrm{O} + \mathrm{e}^+ + \nu \\
{}^{17}\mathrm{O} + {}^{1}\mathrm{H} &\rightarrow {}^{14}\mathrm{N} + {}^{4}\mathrm{He}
\end{aligned} \tag{6.48}$$

[1] For example, if we denote by r_{pD} the rate of $^2\mathrm{H} + {}^1\mathrm{H}$, one has $r_{\mathrm{pD}} = r_{\mathrm{pp}}$, etc. Note that describing the p-p reaction as 'slow' and the $^2\mathrm{H} + {}^1\mathrm{H}$ as 'fast' refers to the difference in cross-section factors $\langle \sigma \upsilon \rangle$ and not to the number of reactions per second r given by eq. (6.8).

The ^{12}C nucleus is reproduced after the first six reactions, and thus only acts as a catalyst for the net hydrogen burning reaction (6.44). This set of six reactions forms the main cycle, also called the CN cycle. The ^{15}N + ^{1}H reaction has a small probability (somewhat less than 10^{-3}) to produce ^{16}O instead of ^{12}C + ^{4}He. This opens up a branching into the second cycle indicated in (6.48). The last three reactions have the effect of transforming ^{16}O, which is initially very abundant, into ^{14}N and thus bringing it into the main CN cycle. The relative proportions of C, N and O nuclei in the cycles change according to the different speeds of the reactions involved, but the total number of CNO-nuclei is always conserved. The three β-decay reactions have neutrino energies between 0.71 and 1.00 MeV and decay times between 10^2 and 10^3 sec. Unless very rapid changes are considered, these β-decays are so fast that one can ignore their detailed rates and the small resulting abundances of ^{13}N, ^{15}O and ^{17}F.

At high enough temperatures, $T \gtrsim 1.5 \times 10^7$ K, all reactions in the cycle come into a steady state or 'equilibrium' where the rate of production of each nucleus equals its rate of consumption. In this situation, as was the case with the p-p chain, the speed of the whole CNO cycle is controlled by the slowest reaction (the one with the smallest cross-section) which is ^{14}N(p, γ)^{15}O. This reaction acts like a bottleneck that congests the nuclei in their flow through the cycle, and ^{14}N thus becomes by far the most abundant of all the CNO nuclei. Looking at this in a bit more detail, the speed of the different reactions in the cycle can be expressed in terms of the nuclear lifetimes $\tau_{\rm p}$ against proton captures, as defined in eq. (6.39). In equilibrium one has d$n(^{12}\mathrm{C})/\mathrm{d}t$ = d$n(^{13}\mathrm{C})/\mathrm{d}t$, etc., so that

$$\left[\frac{n(^{12}\mathrm{C})}{n(^{13}\mathrm{C})}\right]_{\rm eq} = \frac{\langle\sigma v\rangle_{13}}{\langle\sigma v\rangle_{12}} = \frac{\tau_{\rm p}(^{12}\mathrm{C})}{\tau_{\rm p}(^{13}\mathrm{C})}\,, \qquad \text{etc.} \tag{6.49}$$

For the reactions in the CN cycle one typically has

$$\tau_{\rm p}(^{15}\mathrm{N}) \ll \tau_{\rm p}(^{13}\mathrm{C}) < \tau_{\rm p}(^{12}\mathrm{C}) \ll \tau_{\rm p}(^{14}\mathrm{N}) \ll \tau_{\rm nuc}\,.$$

Thus nearly all initially present CNO nuclei are transformed into ^{14}N by the CNO cycle. Therefore, apart from ^{4}He, the second-most important product of the CNO-cycle is ^{14}N – especially because the gas out of which stars form is typically more abundant in carbon and oxygen than in nitrogen.

The energy generation rate of the CNO cycle in equilibrium can be written as

$$\epsilon_{\rm CNO} = q_{\rm H}\, X\, X_{14}\, \frac{\rho}{m_{\rm u}}\, \langle\sigma v\rangle_{\rm pN}, \tag{6.50}$$

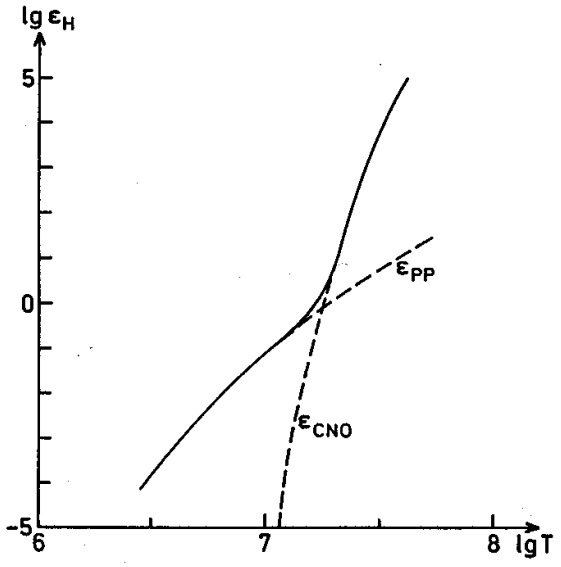

Figure 6.5. Total energy generation rate $\epsilon_{\rm H}$ (in erg g^{-1} s^{-1}) for hydrogen burning as a function of temperature, for ρ = 1 g/cm^3 and abundances X = 1 and $X_{\rm CNO}$ = 0.01. The dashed curves show the contributions of the pp chain and the CNO cycle. Figure from KIPPENHAHN.

where $\langle\sigma v\rangle_{\rm pN}$ is the cross-section factor of the ^{14}N(p, γ)^{15}O reaction which controls the rate of the whole cycle. X_{14} is the ^{14}N mass fraction in the energy-generating zone of the star, which is close to the total abundance $X_{\rm CNO}$ of CNO nuclei once equilibrium is reached in the full CNO cycle. The energy release per unit mass $q_{\rm H} = Q_{\rm H}/4m_{\rm u}$ takes into account the neutrino losses, which for the CNO cycle in equilibrium amounts to $Q_{\rm H} = 24.97$ MeV. The temperature sensitivity of the CNO cycle is much higher than for the pp chain, with ν varying between 23 and 13 for T_7 ranging from 1.0 to 5.0. This is illustrated in Fig. 6.5 where the temperature dependence of $\epsilon_{\rm CNO}$ is compared to that of $\epsilon_{\rm pp}$. For the purpose of very simple approximations one can take

$$\epsilon_{\rm pp} \propto X^2 \rho\, T^4 \qquad \text{and} \qquad \epsilon_{\rm CNO} \propto X X_{14} \rho\, T^{18}. \tag{6.51}$$

The strong difference in temperature sensitivity has the consequence that the pp chain dominates at low temperatures, $T_7 \lesssim 1.5$, while the CNO cycle is dominant at higher temperatures.

6.4.2 Helium burning

Helium burning consists of the fusion of ^{4}He into a mixture of ^{12}C and ^{16}O, which takes place at temperatures $T \gtrsim 10^8$ K. Such high temperatures are needed because (1) the Coulomb barrier for He fusion is higher than that of the H-burning reactions considered above, and (2) fusion of ^{4}He is hindered by the fact that no stable nucleus exists with mass number $A = 8$. Therefore helium burning must occur in two steps:

$$\begin{aligned} &^4\mathrm{He} + {}^4\mathrm{He} \leftrightarrow {}^8\mathrm{Be} \\ &^8\mathrm{Be} + {}^4\mathrm{He} \rightarrow {}^{12}\mathrm{C}^* \rightarrow {}^{12}\mathrm{C} + \gamma \end{aligned} \tag{6.52}$$

The ^{8}Be nucleus temporarily formed in the first reaction has a ground state that is 92 keV higher in energy than that of two separate ^{4}He nuclei. It therefore decays back into two α particles after a few time 10^{-16} s. While extremely short, this time is long enough to build up a very small equilibrium concentration of ^{8}Be, which increases with temperature and reaches about 10^{-9} at $T \approx 10^8$ K. Then the second reaction ^{8}Be(α, γ)^{12}C starts to occur at a significant rate, because of a resonance at just the Gamow peak energy. The result is an excited compound nucleus ^{12}C* which subsequently decays to the ground state of ^{12}C with emission of a γ photon. The corresponding energy level in the ^{12}C nucleus was predicted by Fred Hoyle in 1954, because he could not otherwise explain the existence of large amounts of carbon in the Universe. This excited state of ^{12}C was subsequently found in laboratory experiments.

The net effect of the two reactions (6.52) is called the *triple-α* reaction,

$$3\,{}^4\mathrm{He} \rightarrow {}^{12}\mathrm{C} + \gamma, \tag{6.53}$$

which has $Q = 7.275$ MeV. The energy release per unit mass is $q_{3\alpha} = Q/m(^{12}\mathrm{C}) = 5.9 \times 10^{17}$ erg/g, which is about 1/10 smaller than for H-burning. Since the two reactions need to occur almost simultaneously, the 3α reaction behaves as if it were a three-particle reaction and its rate is proportional to n_α^3. The energy-generation rate can be written as

$$\epsilon_{3\alpha} = q_{3\alpha}\, X_4^3 \rho^2\, \lambda_{3\alpha}, \tag{6.54}$$

where the temperature dependence is described by the factor $\lambda_{3\alpha}$, which depends on the combined cross-sections of the two reactions (6.52). $X_4 \approx Y$ is the mass fraction of ^{4}He. The temperature sensitivity of the 3α rate is extremely high, with $\nu \approx 40$ at $T_8 \approx 1.0$.

When a sufficient amount of ^{12}C has been created by the 3α reaction, it can capture a further α particle to form ^{16}O,

$$^{12}\mathrm{C} + {}^4\mathrm{He} \rightarrow {}^{16}\mathrm{O} + \gamma, \tag{6.55}$$

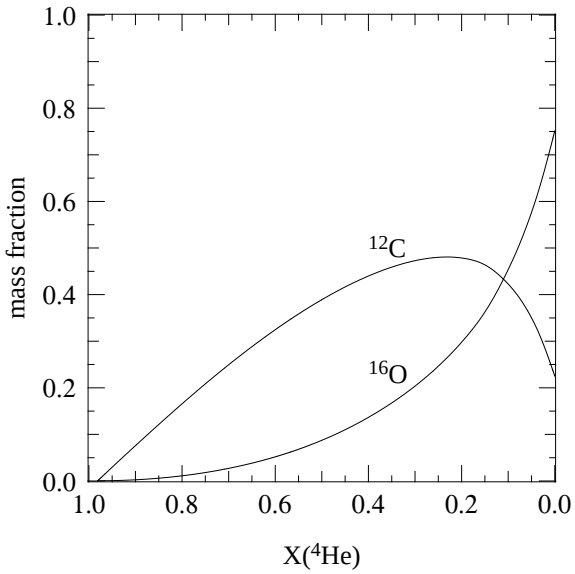

Figure 6.6. Dependence of the mass fractions of ^{12}C and ^{16}O on ^{4}He during He-burning, for typical conditions in intermediate-mass stars.

which has $Q = 7.162\,\mathrm{MeV}$, or $q_{\alpha C} = 4.32 \times 10^{17}$ erg per gram of produced ^{16}O. In principle further α captures on ^{16}O are possible, forming ^{20}Ne, but during normal helium burning conditions these are very rare. The $^{12}\mathrm{C}(\alpha,\gamma)^{16}\mathrm{O}$ reaction is strongly affected by resonances and its rate is quite uncertain. This is important because this reaction competes with the 3α reaction for available ^{4}He nuclei, as illustrated by Fig. 6.6. The final $^{12}\mathrm{C}/^{16}\mathrm{O}$ ratio reached at the end of He-burning is therefore also uncertain.

6.4.3 Carbon burning and beyond

In the mixture of mainly ^{12}C and ^{16}O that is left after helium burning, further fusion reactions can occur if the temperature rises sufficiently. In order of increasing temperature, the nuclear burning cycles that may follow are the following.

Carbon burning When the temperature exceeds $T_8 \gtrsim 5$ the large Coulomb barrier for $^{12}\mathrm{C} + {}^{12}\mathrm{C}$ fusion can be overcome. This is a complicated reaction, in which first an excited compound ^{24}Mg nucleus is formed which can then decay via many different channels. The most important channels are the following:

$$\begin{aligned} {}^{12}\mathrm{C} + {}^{12}\mathrm{C} \rightarrow {}^{24}\mathrm{Mg}^* &\rightarrow {}^{20}\mathrm{Ne} + \alpha \qquad Q = 4.616\,\mathrm{MeV} \quad (\sim 50\%) \\ &\rightarrow {}^{23}\mathrm{Na} + \mathrm{p} \qquad Q = 2.238\,\mathrm{MeV} \quad (\sim 50\%) \end{aligned} \tag{6.56}$$

The protons and α particles released find themselves at extremely high temperatures compared to those needed for hydrogen and helium burning, and will almost immediately react with other nuclei in the mixture, from ^{12}C to ^{24}Mg. Examples are $^{23}\mathrm{Na}(\mathrm{p},\alpha)^{20}\mathrm{Ne}$, $^{20}\mathrm{Ne}(\alpha,\gamma)^{24}\mathrm{Mg}$ and chains such as $^{12}\mathrm{C}(\mathrm{p},\gamma)^{13}\mathrm{N}(\mathrm{e}^+\nu)^{13}\mathrm{C}(\alpha,\mathrm{n})^{16}\mathrm{O}$, where the neutron will immediately react further. The overall energy release is obtained from the combination of all these reactions and is roughly $Q \approx 13\,\mathrm{MeV}$ per $^{12}\mathrm{C}+{}^{12}\mathrm{C}$ reaction. The main products after exhaustion of all carbon are ^{16}O, ^{20}Ne and ^{24}Mg (together 95% by mass fraction). These most abundant nuclei have equal numbers of protons and neutron, but some of the side reactions produce neutron-rich isotopes like ^{21,22}Ne, ^{23}Na and ^{25,26}Mg, so that after C burning the overall composition has a 'neutron excess' (n/p > 1, or $\mu_e > 2$).

Neon burning The next nuclear burning cycle might be expected to be oxygen fusion, but already at somewhat lower temperature ($T_9 \approx 1.5$) a process called 'neon burning' is initiated by the photo-disintegration of ^{20}Ne. At this temperature a sufficient number of photons have energies in the MeV range which is sufficient to break up the relatively fragile ^{20}Ne nucleus into ^{16}O and ^{4}He. This is immediately followed by the capture of the α particle by another ^{20}Ne nucleus, thus:

$$\begin{aligned} &^{20}\mathrm{Ne} + \gamma \leftrightarrow {}^{16}\mathrm{O} + \alpha \qquad Q = -4.73\,\mathrm{MeV} \\ &^{20}\mathrm{Ne} + \alpha \rightarrow {}^{24}\mathrm{Mg} + \gamma \qquad Q = 9.31\,\mathrm{MeV} \end{aligned} \tag{6.57}$$

The first reaction is endothermic, but effectively the two reactions combine to $2\,{}^{20}\mathrm{Ne} \rightarrow {}^{16}\mathrm{O} + {}^{24}\mathrm{Mg}$ with a net energy release $Q > 0$. The composition after neon burning is mostly ^{16}O and ^{24}Mg (together 95% by mass fraction).

Oxygen burning At $T_9 \approx 2.0$ fusion of ^{16}O nuclei sets in, which is in many ways analogous to the carbon fusion reaction described above. Also in this case there are several reaction channels, the most important ones being:

$$\begin{aligned} {}^{16}\mathrm{O} + {}^{16}\mathrm{O} \rightarrow {}^{32}\mathrm{S}^* &\rightarrow {}^{28}\mathrm{Si} + \alpha \qquad Q = 9.59\,\mathrm{MeV} \quad (\sim 60\%) \\ &\rightarrow {}^{31}\mathrm{P} + \mathrm{p} \qquad Q = 7.68\,\mathrm{MeV} \quad (\sim 40\%) \end{aligned} \tag{6.58}$$

Similar to carbon burning, the p and α particles are immediately captured by other nuclei, giving rise to a multitude of secondary reactions that eventually lead to a composition mostly consisting of ^{28}Si and ^{32}S (together 90% by mass fraction). The net energy release per ^{16}O + ^{16}O reaction is $Q \approx 16\,\mathrm{MeV}$. Since some of the side reactions involve β^+-decays and electron captures, the neutron excess of the final mixture is further increased.

Silicon burning The lightest and most abundant nucleus in the ashes of oxygen burning is ^{28}Si, but the Coulomb barrier for ^{28}Si + ^{28}Si fusion is prohibitively high. Instead silicon burning proceeds by a series of photo-disintegration (γ, α) and α-capture (α, γ) reactions when $T_9 \gtrsim 3$. Part of the silicon 'melts' into lighter nuclei, while another part captures the released ^{4}He to make heavier nuclei:

$$\begin{aligned} &{}^{28}\mathrm{Si}\,(\gamma,\alpha)\,{}^{24}\mathrm{Mg}\,(\gamma,\alpha)\,{}^{20}\mathrm{Ne}\,(\gamma,\alpha)\,{}^{16}\mathrm{O}\,(\gamma,\alpha)\,{}^{12}\mathrm{C}\,(\gamma,\alpha)\,2\alpha \\ &{}^{28}\mathrm{Si}\,(\alpha,\gamma)\,{}^{32}\mathrm{S}\,(\alpha,\gamma)\,{}^{36}\mathrm{Ar}\,(\alpha,\gamma)\,{}^{40}\mathrm{Ca}\,(\alpha,\gamma)\,{}^{44}\mathrm{Ti}\,(\alpha,\gamma)\,\ldots\,{}^{56}\mathrm{Ni} \end{aligned} \tag{6.59}$$

Most of these reactions are in equilibrium with each other, e.g. $^{28}\mathrm{Si} + \gamma \leftrightarrow {}^{24}\mathrm{Mg} + \alpha$, and the abundances of the nuclei can be described by nuclear equivalents of the Saha equation for ionization equilibrium. For $T > 4 \times 10^9\,\mathrm{K}$ a state close to *nuclear statistical equilibrium (NSE)* can be reached, where the most abundant nuclei are those with the lowest binding energy, constrained by the total number of neutrons and protons present. The final composition is then mostly ^{56}Fe because n/p > 1 (due to β-decays and e^--captures during previous burning cycles).

6.5 Neutrino emission

Neutrinos play a special role because their cross-section for interaction with normal matter is extremely small. The neutrinos that are released as a by-product of nuclear reactions have typical energies in the MeV range, and at such energies the interaction cross-section is $\sigma_\nu \sim 10^{-44}\,\mathrm{cm}^2$. The corresponding mean free path in matter at density $\rho = n\mu m_\mathrm{u}$ is $\ell_\nu = 1/(n\sigma_\nu) = \mu m_\mathrm{u}/(\rho\sigma_\nu) \sim 2 \times 10^{20}\,\mathrm{cm}/\rho$, for $\mu \approx 1$. Even at densities as high as $10^6\,\mathrm{g/cm}^3$, this gives $\ell_\nu \sim 3000\,R_\odot$. Therefore

any neutrino produced in the interior of a normal star leaves the star without interaction, carrying away its energy. The energy of neutrinos therefore has to be treated separately from other forms of energy, which are transported by a diffusive process due to a temperature gradient.

As mentioned before, the energy loss by neutrinos that are produced in nuclear reactions are conventionally taken into account by subtracting the neutrino energy from the total energy release of a reaction. In other words, the $\epsilon_{\rm nuc}$ term in the energy balance equation (5.4) is reduced and no separate ϵ_ν term is needed for these neutrinos.

However, also in the absence of nuclear reactions, *spontaneous neutrino emission* can occur at high densities and temperatures as a result of weak interaction processes. Owing to the fundamental coupling of the electromagnetic and weak interactions, for each electronic process that emits a photon, there is a very small but finite probability of emitting a neutrino-antineutrino pair instead of a photon. The theory of weak interactions predicts this probability to be

$$\frac{P(\nu\bar{\nu})}{P(\gamma)} \approx 3 \times 10^{-18} \left(\frac{E_\nu}{m_{\rm e} c^2} \right)^4, \tag{6.60}$$

where E_ν is the neutrino energy. These $\nu\bar{\nu}$ emissions represent a direct loss of energy from the stellar interior (a positive ϵ_ν in eq. 5.4) and thus give rise to *cooling* of the stellar matter.

The following processes of this type are important in stellar interiors (see Maeder Sec. 9.5 or Kippenhahn Sec. 18.6 for more details):

Photo-neutrinos In the process of electron scattering, discussed in Sec. 5.3.1, a photon is scattered by a free electron. There is a tiny probability (6.60) that the outgoing photon is replaced by a neutrino-antineutrino pair: $\gamma + {\rm e}^- \rightarrow {\rm e}^- + \nu + \bar{\nu}$. The average neutrino energy is $E_\nu \sim kT$, and therefore the probability of producing a $\nu\bar{\nu}$ pair instead of a photon is proportional to T^4. The rate of neutrino emission is also proportional to the number density of photons, $n_\gamma \propto T^3$, so that ϵ_ν is a very strong function of temperature, roughly $\epsilon_\nu \propto T^8$. The process of photo-neutrino emission results in significant cooling of stellar matter at $T \gtrsim 2 \times 10^8$ K.

Pair annihilation neutrinos At temperatures, $T \gtrsim 10^9$ K, energetic photons can undergo pair creation (Sec. 3.6.2), quickly followed by annihilation of the electron-positron pair. This normally yields two photons and these processes reach an equilibrium ($\gamma + \gamma \leftrightarrow {\rm e}^+ + {\rm e}^-$). Once in every $\sim 10^{19}$ cases, however, the annihilation produces a neutrino-antineutrino pair: ${\rm e}^+ + {\rm e}^- \rightarrow \nu + \bar{\nu}$, which results in a small one-way leakage out of the equilibrium exchange. This represents an important energy loss in a very hot, but not too dense plasma (ϵ_ν increases even more strongly with T than for photo-neutrinos, but is inversely proportional to ρ).

Plasma-neutrinos In a dense plasma, an electromagnetic wave can generate collective oscillations of the electrons. The energy of these waves is quantized and a quantum of this oscillation energy is called a 'plasmon'. The plasmon usually decays into photons, but again there is a finite probability (6.60) of $\nu\bar{\nu}$ emission. This process of neutrino energy loss dominates at high density, when the electron gas is degenerate.

Bremsstrahlung neutrinos Bremsstrahlung is the emission of a photon by an electron that is slowed down in the Coulomb field of an atomic nucleus (the inverse of free-free absorption, Sec. 5.3.1). The small probability of $\nu\bar{\nu}$ emission instead of a photon gives rise to significant cooling at low temperature and very high density. Unlike the processes discussed above, Bremsstrahlung depends on the presence of nuclei and therefore is more efficient for heavy elements (the neutrino emission rate is $\propto Z^2/A$).

The Urca process This process is different from the ones discussed above in that it involves nuclear transformations. Certain nuclei (Z, A) can capture an electron and subsequently undergo a β-decay back to the original nucleus,

$$\begin{aligned}(Z, A) + \mathrm{e}^- &\rightarrow (Z-1, A) + \nu \\ (Z-1, A) &\rightarrow (Z, A) + \mathrm{e}^- + \bar{\nu}.\end{aligned} \tag{6.61}$$

The net result is that the original particles are restored and two neutrinos are emitted. Only certain nuclei are suitable for this process: the nucleus $(Z-1, A)$ must be β-unstable and have a slightly higher rest energy than (Z, A), and the captured electron must be energetic enough to make the first reaction possible. These conditions are quite restrictive and the Urca process is inconsequential under most conditions found in stars, but it can play a role in very late stages of evolution at very high densities.

Suggestions for further reading

The contents of this chapter are also covered by Chapter 9 of MAEDER and by Chapter 18 of KIPPENHAHN.

Exercises

6.1 Conceptual questions: Gamow peak

N.B. Discuss your answers to this question with your fellow students or with the assistant.

In the lecture (see eq. 6.22) you saw that the reaction rate is proportional to

$$\langle \sigma \upsilon \rangle = \left(\frac{8}{m\pi}\right)^{1/2} \frac{S(E_0)}{(kT)^{3/2}} \int_0^\infty e^{-E/kT} e^{-b/E^{1/2}} dE,$$

where the factor $b = \pi(2m)^{1/2} Z_1 Z_2 e^2/\hbar$, and $m = m_1 m_2/(m_1 + m_2)$ is the reduced mass.

(a) Explain in general terms the meaning of the terms $e^{-E/kT}$ and $e^{-b/E^{1/2}}$.

(b) Sketch both terms as function of E. Also sketch the product of both terms.

(c) The reaction rate is proportional to the area under the product of the two terms. Draw a similar sketch as in question (b) but now for a higher temperature. Explain why and how the reaction rate depends on the temperature.

(d) Explain why hydrogen burning can take place at lower temperatures than helium burning.

(e) Elements more massive than iron, can be produced by neutron captures. Neutron captures can take place at low temperatures (even at terrestrial temperatures). Can you explain why?

6.2 Hydrogen burning

(a) Calculate the energy released per reaction in MeV (the Q-value) for the three reactions in the pp1 chain. (Hint: first calculate the equivalent of $m_\mathrm{u}c^2$ in MeV.)

(b) What is the total effective Q-value for the conversion of four ^{1}H nuclei into ^{4}He by the pp1 chain? Note that in the first reaction ($^1\mathrm{H} + {}^1\mathrm{H} \rightarrow {}^2\mathrm{H} + \mathrm{e}^+ + \nu$) a neutrino is released with (on average) an energy of 0.263 MeV.

(c) Calculate the energy released by the pp1 chain in erg/g.

(d) Will the answer you get in (c) be different for the pp2 chain, the pp3 chain or the CNO cycle? If so, why? If not, why not?

6.3 Relative abundances for CN equilibrium

Estimate the relative abundances of the nuclei CN-equilibrium if their lifetimes against proton capture at $T = 2 \times 10^7$ K are: $\tau_p(^{15}\mathrm{N}) = 30$ yr, $\tau_p(^{13}\mathrm{C}) = 1600$ yr, $\tau_p(^{12}\mathrm{C}) = 6600$ yr and $\tau_p(^{14}\mathrm{N}) = 6 \times 10^5$ yr.

6.4 Helium burning

(a) Calculate the energy released per gram for He burning by the 3α reaction and the $^{12}\mathrm{C} + \alpha$ reaction, if the final result is a mixture of 50% carbon and 50% oxygen (by mass fraction).

(b) Compare the answer to that for H-burning. How is this related to the duration of the He-burning phase, compared to the main-sequence phase?

6.5 Comparing radiative and convective cores

Consider a H-burning star of mass $M = 3M_\odot$, with a luminosity L of $80L_\odot$, and an initial composition $X = 0.7$ and $Z = 0.02$. The nuclear energy is generated only in the central 10% of the mass, and the energy generation rate per unit mass, ϵ_{nuc}, depends on the mass coordinate as

$$\epsilon_{nuc} = \epsilon_c \left(1 - \frac{m}{0.1M}\right)$$

(a) Calculate and draw the luminosity profile, l, as a function of the mass, m. Express ϵ_c in terms of the known quantities for the star.

(b) Assume that all the energy is transported by radiation. Calculate the H-abundance as a function of mass and time, $X = X(m, t)$. What is the central value for X after 100 Myr? Draw X as a function of m. (Hint: the energy generation per unit mass is $Q = 6.3 \times 10^{18}$ erg g^{-1}).

(c) In reality, ϵ_{nuc} is so high that the inner 20% of the mass is unstable to convection. Now, answer the same question as in (b) and draw the new X profile as a function of m. By how much is the central H-burning lifetime extended as a result of convection?